

SAMPLE COMPLEXITY ANALYSIS OF MULTI-TARGET DETECTION VIA MARKOVIAN AND HARD-CORE MULTI-REFERENCE ALIGNMENT

KWEKU ABRAHAM, AMNON BALANOV, TAMIR BENDORY, AND CARLOS ESTEVE-YAGÜE

ABSTRACT. Motivated by single-particle cryo-electron microscopy, we study the sample complexity of the multi-target detection (MTD) problem, in which an unknown signal appears multiple times at unknown locations within a long, noisy observation. We propose a patching scheme that reduces MTD to a non-i.i.d. multi-reference alignment (MRA) model. In the one-dimensional setting, the latent group elements form a Markov chain, and we show that the convergence rate of any estimator matches that of the corresponding i.i.d. MRA model, up to a logarithmic factor in the number of patches. Moreover, for estimators based on empirical averaging, such as the method of moments, the convergence rates are identical in both settings. We further establish an analogous result in two dimensions, where the latent structure arises from an exponentially mixing random field generated by a hard-core placement model. As a consequence, if the signal in the corresponding i.i.d. MRA model is determined by moments up to order n_{\min} , then in the low-SNR regime the number of patches required to estimate the signal in the MTD model scales as $\sigma^{2n_{\min}}$, where σ^2 denotes the noise variance.

1. INTRODUCTION

1.1. Problem formulation. In this work, we analyze the sample complexity of the *multi-target detection* (MTD) problem. The goal is to recover a signal $X \in \mathbb{R}^L$ that appears multiple times at unknown locations within a noisy observation $Z \in \mathbb{R}^{LM}$ [12]. The observation model is

$$(1) \quad Z = \sum_{i=1}^q S(t_i) * X + \varepsilon,$$

where $*$ denotes linear convolution, q is the number of signal occurrences, and $\varepsilon \sim \mathcal{N}(0, \sigma^2 I_{LM})$ is additive Gaussian noise. Each unknown location $t_i \in \{0, 1, \dots, LM - 1\}$ is represented by a one-hot vector $S(t_i) \in \{0, 1\}^{LM}$, which shifts X so that its first entry is aligned at position t_i in Z . While both the signal X and the set of positions $\{t_i\}_{i=1}^q$ are unknown, we treat the positions as nuisance parameters and focus on estimating X . Throughout the introduction, we describe the one-dimensional MTD model with $X \in \mathbb{R}^L$ and measurement $Z \in \mathbb{R}^{LM}$ for clarity of exposition. However, our main results also apply in a two-dimensional setting, where the signal is $X \in \mathbb{R}^{L \times L}$ and the measurement is $Z \in \mathbb{R}^{ML \times ML}$. This extension is introduced in Section 5.2.

At low noise levels, signal occurrences can be reliably detected and aligned, allowing for averaging to suppress noise and improve recovery [21]. However, as the noise level increases, localizing signal instances becomes increasingly unreliable. In such high-noise regimes, one must estimate the underlying signal without access to positional information (see Figure 1(a) for illustration). This

Date: December 16, 2025.

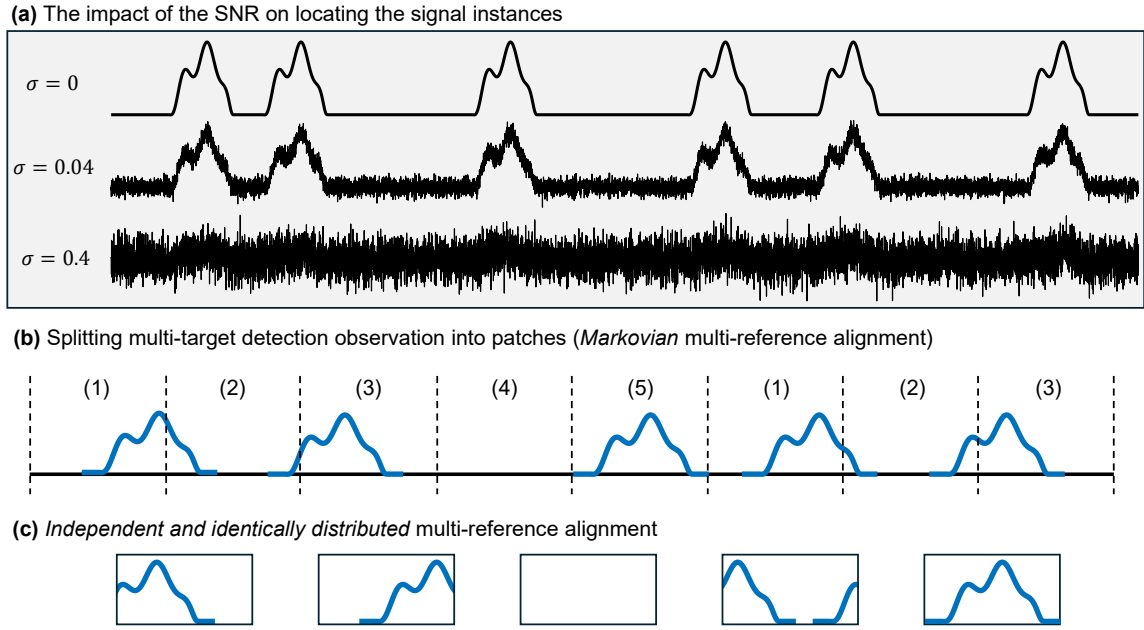


FIGURE 1. **The multi-target detection (MTD) model, and its relation to the Markovian and i.i.d. multi-reference alignment (MRA) models in one dimension.** (a) The MTD model contains signal instances that are embedded at random locations within a noisy observation. In the low-noise regime, it is possible to identify the locations of these instances. However, in the high-noise regime, which is our motivation in this work, the signal locations cannot be reliably recovered. (b) To address this challenge, we divide the MTD observation into non-overlapping patches. These patches form what we call the *Markovian MRA* model, where adjacent patches exhibit statistical Markovian dependencies. Each patch can take one of five possible forms: (1) a cropped prefix of a signal instance; (2) two cropped segments, consisting of the suffix of one signal instance followed by the prefix of another; (3) a cropped suffix of a signal instance; (4) an empty patch; or (5) a complete signal instance. (c) In contrast, the *i.i.d. MRA* model assumes the patches are independent and identically distributed, with no statistical dependency between them. A central contribution of this work is establishing a connection between the Markovian MRA model and the *i.i.d.* MRA model, enabling analysis via known tools and results for the *i.i.d.* case.

work aims to characterize the sample complexity of the MTD model, namely the observation length (LM) needed to recover the underlying signal reliably, in the presence of high noise.

1.2. Motivating application: Cryo-electron microscopy. The primary motivation for the MTD model arises in cryo-electron microscopy (cryo-EM) [33, 11, 36] and cryo-electron tomography (cryo-ET) [19, 35, 41]. Over the past decade, single-particle cryo-EM has become a leading method

for determining the spatial structures of biological macromolecules, particularly proteins [5, 24, 20]. It enables reconstruction of molecular structures in their native state and has achieved atomic-level resolution for numerous proteins. Beyond static structure determination, cryo-EM also offers the potential to capture conformational dynamics, which are critical for understanding protein function [37].

In a cryo-EM experiment, dozens of micrographs are recorded, each containing multiple 2D projections of an unknown 3D molecular structure at unknown orientations and positions. To avoid radiation damage, imaging is performed under extremely low electron doses, yielding a very low signal-to-noise ratio (SNR), often around 1/100 [11]. The central challenge is to reconstruct the 3D structure from these noisy projections without knowledge of their locations or viewing directions. As the molecular size decreases, the SNR drops further, making particle detection increasingly difficult and, in extreme cases, infeasible [27]. Under such low-SNR conditions, downstream analyses can be strongly affected, sometimes producing misleading structural inferences [28, 8].

The MTD framework was recently proposed as a computational approach for recovering small structures that lie beyond the capabilities of current methodologies. Although heuristic algorithms have been developed, most notably those based on the method of moments and approximate expectation–maximization [13, 29, 12], the theoretical and statistical foundations of signal recovery in this regime remain largely unexplored [7]. To be more precise, some statistical properties of cryo-EM have been analyzed in [9, 16, 15], under the assumption that particle locations are known. However, the full problem with *unknown locations* has not been addressed, and the present work constitutes a first step toward this more general and realistic formulation.

The MTD model analyzed in this work (1) serves as a simplified abstraction of the signal-recovery process underlying the cryo-EM computational problem. Specifically, it isolates the challenge of unknown translations while omitting other sources of uncertainty that arise in more realistic settings, such as rotational variability and tomographic projection effects. This simplification allows us to focus on the core statistical and computational difficulties of recovery in the low-SNR regime under unknown locations of the signal instances, while serving as a first step toward more advanced models that more closely reflect cryo-EM. In Section 7, we discuss how the insights developed here could extend to more general models, including those directly relevant to cryo-EM.

1.3. Signal recovery using Markovian modeling. In this work, we develop an estimation framework based on patch extraction and Markovian modeling, illustrated in Figure 1(b). The central idea is to recover X by dividing the long MTD measurement Z (defined in (1)) into M non-overlapping patches, each of length L . These patches, denoted by $\{Z_k\}_{k=1}^M \subset \mathbb{R}^L$, are defined by

$$(2) \quad Z_k[\xi] := Z[L(k-1) + \xi], \quad \text{for } \xi \in \{0, \dots, L-1\}, \quad k = 1, \dots, M.$$

1.3.1. Description of each patch. Under the non-overlapping assumption, where no two signal instances share overlapping coordinates, each patch has five possible forms: (i) a cropped prefix of a signal instance; (ii) two cropped segments, consisting of the suffix of one signal instance followed by the prefix of another; (iii) a cropped suffix of a signal instance; (iv) an empty patch; or (v) a complete signal instance. Let $i_k^{(0)}, i_k^{(1)} \in \{0, \dots, L\}$ denote the starting indices of the possible occurrence of X within the patches Z_{k-1} and Z_k respectively, considering $i_k^{(0)} = 0$ in case the patch

Z_{k-1} does not contain the starting pixel of X , and $i_k^{(1)} = L$ in case the patch Z_k does not contain the starting pixel of X . The non-overlapping condition is equivalent to $i_k^{(1)} \geq i_k^{(0)}$. We define the padded version of X given by $\tilde{X} = [X, 0_L]$, where $0_L \in \mathbb{R}^L$ denotes the vector of L zeros. Then, each patch $Z_k \in \mathbb{R}^L$ can be expressed as

$$(3) \quad Z_k[\xi] = \tilde{X} \left[\xi - i_k^{(1)} \bmod 2L \right] + \tilde{X} \left[\xi + L - i_k^{(0)} \right] + \varepsilon_k, \quad \text{for } \xi \in \{0, \dots, L-1\},$$

where $\varepsilon_k \stackrel{i.i.d.}{\sim} \mathcal{N}(0, \sigma^2 I_L)$, $\xi \in \{0, \dots, L-1\}$. Here, $\tilde{X} \left[\xi - i_k^{(1)} \bmod 2L \right]$ corresponds to the prefix entries of the first (possible) instance of X starting in the patch Z_k , while $\tilde{X} \left[\xi + L - i_k^{(0)} \right]$ corresponds to the suffix entries of the (possible) cropped instance of X that started in patch Z_{k-1} . The indices $\{(i_k^{(0)}, i_k^{(1)})\}_{k=1}^M$ are random variables determined by the unknown placements of X in Z , and they introduce statistical dependencies between patches.

1.3.2. *From i.i.d. MRA to Markovian MRA via MTD patches.* The structure of each MTD patch Z_k defined in (3) admits a natural group-theoretic description: a cyclic shift of a zero-padded signal, followed by a linear projection operator. This places the model in direct analogy with the classical i.i.d. *multi-reference alignment (MRA)* problem [10, 9, 14, 6]. In the classical *i.i.d. MRA model*, the task is to estimate $X \in \mathbb{R}^L$ from M independent noisy observations of the form

$$(4) \quad Y_k = P(g_k \cdot X) + \varepsilon_k, \quad g_k \sim \pi, \quad \varepsilon_k \sim \mathcal{N}(0, \sigma^2 I),$$

where g_k is drawn i.i.d. from a distribution π over a compact group G acting on \mathbb{R}^L . A central insight from the MRA literature is that if the orbit of X is uniquely determined by its moments up to order n_{\min} —the *moment order cutoff*—then reliable recovery in the low-SNR regime requires

$$M = \omega(\sigma^{2n_{\min}}),$$

that is, the number of observations must grow faster than $\sigma^{2n_{\min}}$ as $\sigma^2 \rightarrow \infty$ [2].

In contrast, *MTD patches are not i.i.d.* . Although each Z_k can be written in the MRA form (4), the latent group elements $\{g_k\}_{k=1}^M$ inherit dependencies from the random placement of signals in Z (i.e., the group elements g_k are associated with the indices $(i_k^{(0)}, i_k^{(1)})$), forming a hidden Markov model [18]. This motivates the following generalization.

Definition 1.1 (Markovian and i.i.d. MRA models). *We present two versions of the MRA model:*

- (i) **Markovian MRA model** (MTD model with dependent patches, Figure 1(b)): *Let $\{Z_k\}_{k=1}^M$ denote the sequence of patches extracted from the MTD observation Z , as defined in (2). These patches are statistically dependent, governed by a hidden Markov model [18], induced by the random placement of signals in Z . More precisely, $\{Z_k\}_{k=1}^M$ have the form of (4), with $\{g_k\}_{k=1}^M$ being the first M states of a Markov chain.*
- (ii) **IID MRA model** (model with independent observations, Figure 1(c)): *$\{Y_k\}_{k=1}^M$ generated according to (4), with the parameters $\{g_k\}_{k=1}^M$ sampled i.i.d. from a fixed distribution. When this distribution is the stationary distribution of the Markovian MRA model in (i), we refer to it as the induced MRA model.*

Markov chains are among the most fundamental dependent-data models. Under mild conditions, they exhibit *exponential mixing*, meaning that samples taken sufficiently far apart become

nearly independent and approximately follow the stationary distribution [30, 31]. The rate of this convergence is governed by the *absolute spectral gap*, $\Delta = 1 - |\lambda_2|$, where λ_2 is the second-largest eigenvalue of the transition matrix in absolute value. This mixing property will allow us to transfer sample-complexity results from the well-studied i.i.d. MRA to the MTD setting.

Our main results also extend to the two-dimensional setting, motivated by applications in cryo-EM, where the target signal is $X \in \mathbb{R}^{L \times L}$ and the measurement is $Z \in \mathbb{R}^{ML \times ML}$. In this case, the simple Markov description no longer applies. Instead, we adopt a *hard-core model* (see Section 5.2) to describe the spatial distribution of signal occurrences, which retains the essential features of the one-dimensional formulation, while capturing the geometry of the 2D setting.

1.3.3. Main assumptions and relation to prior work. All prior analyses of the MTD model have focused on the *well-separated* regime, in which signal occurrences are assumed to be separated by at least L coordinates [12, 7]. This assumption greatly simplifies the problem, and under this setting, it has been shown that the sample complexity of the MTD model can be upper bounded by $\omega(\sigma^6)$, via explicit recovery from third-order moments [12]. However, it remains unclear whether such guarantees continue to hold in more general settings that relax the separation condition, namely, when signal occurrences do not overlap but are otherwise arbitrarily positioned.

In this work, we focus on the more challenging *non-overlapping* regime, where signal instances may appear arbitrarily close to each other, subject only to the condition that they do not overlap. For the one-dimensional MTD problem, we model the distances between consecutive signal occurrences as independent draws from a Geometric distribution with parameter $\lambda \in (0, 1)$. This assumption is natural for modeling sparsely distributed particles and is essential for endowing the resulting process with a Markov structure. We emphasize that key parts of our analysis, most notably Theorem 3.4, remain valid under weaker conditions, requiring only that patches sufficiently far apart exert limited statistical influence on each other (see Definition 5.5). A natural extension to two dimensions is obtained by assuming a *hard-core* spatial model, in which the same principle of weak long-range correlations ensures that distant patches exert only limited statistical influence on each other (Sections 5–6).

1.4. Main contributions. Our main results establish a direct connection between the sample complexity of the MTD model (Definition 1.1(i)) and that of the i.i.d. MRA model (Definition 1.1(ii)). We show that under natural mixing conditions, the sample complexity of MTD is no greater than that of its corresponding i.i.d. MRA, up to a possible logarithmic factor. In particular, under the assumptions in Section 1.3.3 for the 1D and 2D MTD models, we are able to prove the following:

- (i) *Structure of extracted patches.* In Theorem 3.4 (for the 1D case) and Theorem 6.2 (for the 2D case), we show that the patches $\{Z_k\}_{k=1}^M$ extracted from the MTD measurement admit an MRA-type representation. In the 1D case, this representation takes the exact form of (4) with $X \in \mathbb{R}^L$, and the group elements $\{g_k\}_{k=1}^M$ being the first M states of a Markov chain with positive absolute spectral gap. In the 2D case, where the signal is $X \in \mathbb{R}^{L \times L}$, the representation is a natural two-dimensional analogue of (4); here the group elements follow a stochastic process that satisfies a strong mixing property.
- (ii) *Sample complexity equivalence.* In Theorem 4.2 (for the 1D case) and Theorem 6.3 (for the 2D case), we show that the convergence rate of any estimator under the Markovian MRA model matches the rate under the i.i.d. MRA model, up to a logarithmic factor in

the number of patches M . Moreover, when the estimator is based on empirical averaging, the convergence rates in the two settings match up to a constant factor.

These results imply that, under the stated assumptions, the sample complexity of the MTD model is no greater than that of its associated i.i.d. MRA model. In particular, if orbit recovery for the associated i.i.d. MRA model is possible from n_{\min} -th order moments with sample complexity $\omega(\sigma^{2n_{\min}})$, then the same bound holds for the MTD model.

1.5. Work structure. The paper is organized as follows. Section 2 introduces the method of moments together with the feature-map framework and estimator definitions that we use throughout. Section 3 develops the one-dimensional MTD model: we formalize the measurement model, split it into patches, and show that the induced sequence of patches forms a Markovian MRA model (Theorem 3.4). Section 4 proves that the Markovian MRA model converges to the classical i.i.d. MRA model under exponential mixing time and derives the resulting sample-complexity guarantees; we also state the implications of this result for the method of moments (Corollary 4.3). Section 5 turns to two dimensions, introducing the hard-core placement model, admissibility on the grid graph, and the exponential mixing property for the induced random field. Section 6 establishes the corresponding 2D results: an induced (non-i.i.d.) MRA representation with exponential mixing (Theorem 6.2) and convergence to the i.i.d. MRA setting with matching sample complexity up to logarithmic factors (Theorem 6.3). Finally, Section 7 discusses implications, open questions, and extensions, including algebraic-structure variants and connections to cryo-EM and cryo-ET. All proofs are deferred to the appendices.

2. PRELIMINARIES

The goal of this work is to characterize the sample complexity of the MTD model, defined as the number of patches M needed to reliably recover the signal X in the low-SNR regime. Although the measurement contains q occurrences of X , we express complexity in terms of M . Under our asymptotic framework, the distribution of inter-signal spacings—and hence the stationary law of the induced Markov chain—remains fixed. Equivalently, the density parameter λ , which specifies the expected number of signal occurrences per patch, is treated as constant as $M \rightarrow \infty$. Thus, $q \asymp \lambda M$, so asymptotics in M translate directly to asymptotics in q . The stationary distribution determined by λ governs the typical patch structure and thereby indirectly shapes the sample complexity.

2.1. Method of moments. A key statistical property governing the sample complexity in the i.i.d. MRA model presented in (4) is the moment order cut-off, i.e., the minimal moment order of the observations that uniquely determines the orbit of the signal. We distinguish between two related notions of moments:

- (i) *Noiseless group-transformed moments.* For a compact group G acting on \mathbb{R}^L , let $g \sim \pi$ be a random element drawn from a distribution π over G , and let P be a fixed projection operator. The order- n moment of the noiseless group-transformed signal is

$$(5) \quad M_{X,\pi}^{(n)} \triangleq \mathbb{E}_{g \sim \pi} \left[(P(g \cdot X))^{\otimes n} \right],$$

which captures the n -th order correlations of the projected transformations of X , averaged over the group distribution. Here $v^{\otimes n}$ denotes the n -fold tensor power of a vector $v \in \mathbb{R}^p$, i.e., the rank-one tensor with entries

$$(v^{\otimes n})_{i_1, \dots, i_n} = v_{i_1} \cdots v_{i_n},$$

so that, componentwise,

$$(M_{X, \pi}^{(n)})_{i_1, \dots, i_n} = \mathbb{E}_{g \sim \pi} \left[(P(g \cdot X))_{i_1} \cdots (P(g \cdot X))_{i_n} \right].$$

(ii) *Empirical moments.* In practice, we only observe noisy samples $Y_k = P(g_k \cdot X) + \varepsilon_k$, as defined in (4), and thus the relevant population moment is

$$M_Y^{(n)} \triangleq \mathbb{E}[Y^{\otimes n}] = \mathbb{E}_{g \sim \pi, \varepsilon} \left[(P(g \cdot X) + \varepsilon)^{\otimes n} \right],$$

which depends explicitly on the noise level σ . Given M independent observations $\{Y_k\}_{k=1}^M$, the *empirical n -th moment* is defined as

$$\widehat{M}^{(n)} \triangleq \frac{1}{M} \sum_{k=1}^M (Y_k)^{\otimes n},$$

serving as an estimator of $M_Y^{(n)}$.

A fundamental result in the MRA literature is that if the smallest integer n such that $M_{X, \pi}^{(n)}$ uniquely determines the orbit of X is n_{\min} , then the sample complexity in the low-SNR regime scales as

$$M = \omega(\sigma^{2n_{\min}}).$$

Thus, n_{\min} serves as the key statistical threshold controlling the asymptotic difficulty of orbit recovery.

The minimal moment order n_{\min} (and thus the sample complexity) depends on the group action G , the group distribution π , the projection operator P , and the availability of prior information about X . For example, when $G = \mathbb{Z}_L$ with a uniform distribution π and no prior, recovery requires third-order moments, leading to the scaling $\omega(\sigma^6)$ [14, 9]. In contrast, for generic non-uniform π [1, 17] or when suitable prior information is available [15, 3], second-order moments suffice, reducing the scaling to $\omega(\sigma^4)$. In higher-dimensional settings, such as $G = \text{SO}(3)$ with tomographic projections, the uniform case is also believed to require $n_{\min} = 3$ [9], though the precise characterization remains an open problem.

2.2. Feature maps. To state our main results in a general way, it is useful to introduce the notion of a *feature map*. Formally, a feature map is a function $\mathcal{F} : \mathbb{R}^L \rightarrow \mathbb{R}^d$ that associates to each signal $X \in \mathbb{R}^L$ a vector $\mathcal{F}(X) \in \mathbb{R}^d$ representing the quantities of interest for the estimation task. For instance, if the goal is to characterize the n -th order moment of the observation Y in (4) associated with the underlying signal X , then the feature map is given by

$$(6) \quad \mathcal{F}(X) := \mathbb{E}[Y^{\otimes n}] = \mathbb{E}_{g \sim \pi, \varepsilon} \left[(P(g \cdot X) + \varepsilon)^{\otimes n} \right],$$

which allows recovery of the noiseless moment $M_{X, \pi}^{(n)}$. On the other hand, if the objective is to directly reconstruct X itself, then the natural choice of feature map is the identity transformation $\mathcal{F}(X) \triangleq X$. This general framework allows us to express our results in a way that applies both

to moment-based recovery and to direct signal estimation, thereby unifying the treatment of these problems under a common formalism.

2.2.1. Estimators in Markovian and i.i.d. MRA models. With this formulation of the feature maps, we now extend the definition of the estimators of the Markovian and i.i.d. MRA model introduced in Definition 1.1. Let us denote by

$$(7) \quad \widehat{F} : \bigcup_{M \geq 1} (\mathbb{R}^L)^M \longrightarrow \mathbb{R}^d,$$

any estimator that associates, to any collection of M patches of length L , a prediction of the target features $\mathcal{F}(X)$ of the underlying signal X . Depending on the nature of the patches, we define two estimation models associated to the same map $\widehat{F}(\cdot)$.

Definition 2.1 (Feature estimation in the Markovian and i.i.d. MRA models). *Let $M \in \mathbb{N}$ and let $\widehat{F}(\cdot)$ be the estimator defined in (7), which maps a collection of patches or observations to an approximation of the target features $\mathcal{F}(X) \in \mathbb{R}^d$ of the signal X . We define two associated estimators:*

(i) **Markovian MRA model estimation.** *Given the Markovian model in Definition 1.1(i) and the sequence of patches $\{Z_k\}_{k=1}^M$ extracted from the MTD observation Z , we define, for any $m \in \mathbb{N}$,*

$$\widehat{F}_{\text{MTD}}(M, m) := \widehat{F}(\{Z_{km}\}_{k=1}^{M'}), \quad M' = \lfloor M/m \rfloor,$$

which applies $\widehat{F}(\cdot)$ to a subsampled set of patches, retaining only one out of every m patches to mitigate dependence.

(ii) **i.i.d. MRA model estimation.** *Given the i.i.d. MRA model in Definition 1.1(ii) and the sequence of independent observations $\{Y_k\}_{k=1}^M$, we define*

$$\widehat{F}_{\text{MRA}}(M) := \widehat{F}(\{Y_k\}_{k=1}^M),$$

which applies $\widehat{F}(\cdot)$ directly to the i.i.d. observations.

3. THE ONE-DIMENSIONAL MTD MODEL: FORMING A MARKOVIAN MRA MODEL

This section introduces the preliminaries, definitions, and assumptions underlying the analysis of the one-dimensional MTD model. Section 3.1 presents a detailed formulation of the model, along with the assumption governing the stochastic placement of the signal X within the MTD observation. In Section 3.2, we describe the process of splitting the observation into patches using group actions and projection operators, and in Section 3.3 we establish that the sequence of extracted patches forms a Markovian MRA model.

3.1. The 1-D MTD model.

3.1.1. *Model formulation.* Let $X \in \mathbb{R}^L$ be the signal to be recovered and $Z \in \mathbb{R}^{LM}$ be the measurement introduced in (1). We recall from (1) that the measurement $Z \in \mathbb{R}^{LM}$ is given by

$$Z = \sum_{i=1}^q S(t_i) * X + \varepsilon,$$

where, for each $i \in \{1, \dots, q\}$, the location of the i -th occurrence of the signal X in the measurement is determined by the parameter $t_i \in \{0, \dots, L(M-1)\}$. The linear convolution of the one-hot vector $S(t_i)$ with X is given by

$$(8) \quad S(t_i) * X[\xi] = \begin{cases} X[\xi - t_i], & \xi \in \{t_i, \dots, L-1+t_i\}, \\ 0, & \text{else.} \end{cases}$$

The parameter t_i denotes the location of the first pixel of the i -th occurrence of the signal X , specifically the position of $X[0]$. An example of such a measurement is shown in Figure 1.

3.1.2. *The distribution of signal appearances.* In the 1D MTD model introduced in (1), a natural way to model the distribution of signal appearances is to assume that the number of empty pixels between two consecutive signals follows a geometric distribution with parameter $\lambda \in (0, 1)$, which controls the density of signal occurrences, as we state in the following assumption.

Assumption 3.1 (Distribution of occurrences in 1D MTD model). *The number of empty pixels between two signal appearances follows a zero-indexed Geometric distribution with parameter $\lambda \in (0, 1)$, denoted by $\text{Geo}(\lambda)$, that is, for $k \in \{0, 1, 2, \dots\}$, $\Pr[\text{Geo}(\lambda) = k] = (1 - \lambda)^k \lambda$. The finite set $\{t_i\}_{i=1}^q$ in (1) is generated as the first q terms of the stochastic process*

$$t_1 \sim \text{Geo}(\lambda), \quad t_i - t_{i-1} - L \sim \text{Geo}(\lambda) \quad \forall i = 2, 3, \dots,$$

where

$$q := \max \{i \in \mathbb{N} : t_i \leq L(M-1)\}.$$

It is important to note that this assumption ensures that signal occurrences do not overlap within the measurement. The parameter λ quantifies the density of signal appearances in the MTD measurement: values of λ close to 1 correspond to a high density of X within Z , whereas smaller values of λ indicate sparser occurrences.

3.2. Splitting the measurement into patches. In order to reduce the MTD model to an MRA model, the first step is to divide the measurement into M patches of length L , denoted by $\{Z_k\}_{k=1}^M \subset \mathbb{R}^L$, and given by

$$(9) \quad Z_k[\xi] := Z[L(k-1) + \xi], \quad \text{for all } \xi \in \{0, \dots, L-1\} \text{ and } k = 1, \dots, M.$$

Under the geometric distribution assumption, Assumption 3.1, each patch may contain up to two shifted, non-overlapping instances of the signal $X \in \mathbb{R}^L$. To represent each patch within the MRA framework (as in (3)), next we describe each patch using cyclic shifts and projection operators.

We embed the signal into a zero-padded vector $\tilde{X} := (X, 0_L) \in \mathbb{R}^{2L}$ and consider the action of a finite cyclic group. Consider the cyclic group \mathbb{Z}_{2L} , acting on \mathbb{R}^{2L} by cyclically shifting the coordinates of any vector in \mathbb{R}^{2L} . Specifically, for any $\tilde{g} \in \mathbb{Z}_{2L}$, the group action is defined as:

$$(10) \quad \tilde{g} \cdot \tilde{X}[\xi] = \tilde{X}[\xi - \tilde{g} \bmod 2L], \quad \forall \xi \in \{0, \dots, 2L-1\}.$$

Since each patch can include up to two instances of the signal, we must account for this by defining the relative shift for each instance and applying the appropriate projection. Let \bar{X} represent the concatenation of the two instances:

$$(11) \quad \bar{X} = (\tilde{X}, \tilde{X}) \in \mathbb{R}^{2L} \times \mathbb{R}^{2L}, \quad \text{with } \tilde{X} = [X, 0_L] \in \mathbb{R}^{2L}.$$

Now, consider the direct product group $\mathbb{Z}_{2L} \times \mathbb{Z}_{2L}$, which acts on $\bar{X} \in \mathbb{R}^{2L} \times \mathbb{R}^{2L}$ by applying the group action of \mathbb{Z}_{2L} on each component of \bar{X} . Specifically, for any $g = (g^{(1)}, g^{(2)}) \in \mathbb{Z}_{2L} \times \mathbb{Z}_{2L}$ and any $(\tilde{X}_0, \tilde{X}_1) \in \mathbb{R}^{2L} \times \mathbb{R}^{2L}$, the action is defined as:

$$(12) \quad g \cdot (\tilde{X}_0, \tilde{X}_1) = (g^{(1)}, g^{(2)}) \cdot (\tilde{X}_0, \tilde{X}_1) = (g^{(1)} \cdot \tilde{X}_0, g^{(2)} \cdot \tilde{X}_1).$$

It remains to define the projection operator. We introduce the linear operator $P : \mathbb{R}^{2L} \times \mathbb{R}^{2L} \rightarrow \mathbb{R}^L$ defined as

$$(13) \quad P(\tilde{X}_0, \tilde{X}_1) = P_0 \tilde{X}_0 + P_1 \tilde{X}_1, \quad \text{for any } (\tilde{X}_0, \tilde{X}_1) \in \mathbb{R}^{2L} \times \mathbb{R}^{2L},$$

where $P_0, P_1 : \mathbb{R}^{2L} \rightarrow \mathbb{R}^L$, are linear operators represented by the matrices

$$P_0 = [0_{L \times L} \ I_L] \quad \text{and} \quad P_1 = [I_L \ 0_{L \times L}],$$

with $0_{L \times L}$ denoting the $L \times L$ zero matrix and I_L the identity matrix in \mathbb{R}^L . In words, $P_0 \tilde{X}_0$ extracts the second half of the vector \tilde{X}_0 , while $P_1 \tilde{X}_1$ extracts the first half of the vector \tilde{X}_1 .

3.3. From MTD to a Markovian MRA model. We are now ready to define the MRA model associated with the sequence of patches presented in (9).

Definition 3.2 (The induced MRA model). *Let us consider the finite abelian group $G = \mathbb{Z}_{2L} \times \mathbb{Z}_{2L}$ acting on \bar{X} as described in (12) and (10). Let $P : \mathbb{R}^{2L} \times \mathbb{R}^{2L} \rightarrow \mathbb{R}^L$ be the linear projection operator defined in (13). For a signal $X \in \mathbb{R}^L$, let $\bar{X} \in \mathbb{R}^{2L} \times \mathbb{R}^{2L}$ be defined as in (11). We consider the problem of recovering \bar{X} from noisy group-transformed and projected observations of \bar{X} with the form:*

$$(14) \quad Z_k = P(g_k \cdot \bar{X}) + \varepsilon_k, \quad k \in \{1, 2, \dots, M\},$$

where $\{g_k\}_{k=1}^M \subset G$ is a random variable in the product space $G^M = G \times \dots \times G$, and $\{\varepsilon_k\}_{k=1}^M$ is an i.i.d. noise sequence, $\varepsilon_k \sim \mathcal{N}(0, \sigma^2 I)$.

Remark 3.3 (Recovering X vs. recovering \bar{X}). *Although Definition 3.2 is stated in terms of the lifted object \bar{X} from (11), our ultimate goal is to recover the original signal $X \in \mathbb{R}^L$ (or its features $\mathcal{F}(X)$). By construction, the measurements determine \bar{X} only up to a cyclic shift, reflecting the group action $g_k \cdot \bar{X}$. However, because \bar{X} has the special form of the signal X padded with zeros, this ambiguity can be resolved in a canonical way: the zero-padding breaks the symmetry and uniquely identifies X . Hence, recovery of X from the observations in (14) is well-defined and does not require addressing group invariance. This distinction will be important in the analysis of the mean square error (MSE) for estimators based on the induced MRA model of MTD patches.*

In the following theorem (proved in Appendix A.1), we show that the extracted patches $\{Z_k\}_{k=1}^M$ can be expressed in the form (14), where the sequence $\{g_k\}_{k=1}^M$ forms a Markov chain over the group G .

Theorem 3.4 (Markov structure of the induced model). *Let $L, M \in \mathbb{N}$, and let $X \in \mathbb{R}^L$ be the signal to be recovered. Consider the measurement $Z \in \mathbb{R}^{LM}$ defined by the MTD model in (1), where $q \in \mathbb{N}$ denotes the number of signal occurrences and the placement parameters $\{t_i\}_{i=1}^q$ satisfy Assumption 3.1. Suppose Z is partitioned into M non-overlapping patches $\{Z_k\}_{k=1}^M$ as described in (9). Then, the following holds,*

- (i) *The sequence $\{Z_k\}_{k=1}^M$ can be expressed in the form of Definition 3.2, with associated group elements $\{g_k\}_{k=1}^M = \{(g_k^{(1)}, g_k^{(2)})\}_{k=1}^M$ belonging to the group $G = \mathbb{Z}_{2L} \times \mathbb{Z}_{2L}$.*
- (ii) *The sequence $\{g_k\}_{k=1}^M$ forms a time-homogeneous Markov chain on G .*
- (iii) *There exists a unique stationary distribution π over G such that for any $1 \leq k \leq m \leq M$ and any $g' \in G$, the total variation distance between the conditional distribution of g_m given $g_k = g'$ and the stationary distribution satisfies*

$$(15) \quad \sum_{g \in G} |\mathbb{P}(g_m = g \mid g_k = g') - \pi(g)| \leq C \cdot (1 - (1 - \lambda)^{L-1})^{m-k},$$

for some constant $C > 0$ depending only on λ and L .

3.3.1. *The stationary distribution of the Markov chain.* In Lemma A.1, we prove that the stationary distribution π associated to the Markov chain $\{g_k\}_{k=1}^M$ constructed in the proof of Theorem 3.4 is given explicitly by

$$(16) \quad \pi(x, y) := \begin{cases} \frac{(1 - \lambda)^L}{1 + (L - 1)\lambda} & \text{if } (x, y) = (0, L) \\ \frac{\lambda(1 - \lambda)^{L-x}}{1 + (L - 1)\lambda} & \text{if } 0 < x < L \text{ and } y = L \\ \frac{\lambda(1 - \lambda)^y}{1 + (L - 1)\lambda} & \text{if } x = 0 \text{ and } 0 \leq y < L \\ \frac{\lambda^2(1 - \lambda)^{y-x}}{1 + (L - 1)\lambda} & \text{if } 0 < x \leq y < L \\ 0 & \text{else,} \end{cases}$$

for any $g = (x, y) \in G = \mathbb{Z}_{2L} \times \mathbb{Z}_{2L}$.

Note that, in the definition of π , the five cases correspond, respectively, to (see Figure 1(b) for illustration):

- (i) the probability of a patch not containing any part of the signal X ;
- (ii) the case in which the patch contains only a part of the signal X remaining from the previous patch;
- (iii) the case in which the patch contains only a part of the signal starting in the current patch;
- (iv) the case in which the patch contains two parts of the signal;
- (v) in the last case, if $x > y$, then two instances of the signal X overlap, and thus it has probability 0 due to Assumption 3.1. The cases $x \geq L$ and $y \geq L$ have also probability 0 due to the construction of the Markov chain $g_k = (g_k^{(1)}, g_k^{(2)})$ in the proof of Theorem 3.4 (see the choice of $(g_k^{(1)}, g_k^{(2)})$ in (40) and (41)), which only takes values in $\{0, 1, \dots, L - 1\} \times \{0, 1, \dots, L\}$.

Theorem 3.4 highlights a trade-off governed by the density parameter λ , as seen in the stationary distribution (16). When λ is small, patches frequently contain no signal, so the average number of signal occurrences per patch, equivalently, the *signal density*, is low. This scarcity typically dominates the MSE when the number of patches M is fixed. On the other hand, small λ also implies that signals are far apart, which enhances mixing: most patches are empty, so consecutive patches are nearly independent. Note, however, that a larger λ is generally preferable despite slowing the mixing. The recovery of the underlying signal X relies on the stationary distribution π , and this recovery improves with higher signal density. By contrast, estimation of π itself from the data, which is indeed easier when λ is small, is not the limiting factor from an information-theoretic perspective. We emphasize, however, that, in practical applications, λ is typically dictated by the data generation process and is not under direct control.

4. THE ONE-DIMENSIONAL MTD MODEL: CONVERGENCE TO I.I.D. MRA AND SAMPLE COMPLEXITY

In this section, we show that the Markovian MRA model introduced in Theorem 3.4 converges to the classical i.i.d. MRA model in the limit as the number of patches tends to infinity. Building on this connection, we derive the sample complexity of the Markovian MRA model and compare it to that of its i.i.d. counterpart. Specifically, we use Theorem 3.4 to formally relate the distribution of patches extracted from the MTD measurement to the stationary distribution of the i.i.d. MRA model, in which observations are sampled independently.

As discussed in Section 2.2, a common objective is to estimate specific features of the signal X (e.g., its moments), denoted by $\mathcal{F}(X) \in \mathbb{R}^d$. Let \widehat{F} be the estimator defined in (7), which maps any collection of M patches $\{Z_k\}_{k=1}^M$, each of the form (14), to an estimate of $\mathcal{F}(X)$. Recalling Definition 2.1, we define $\widehat{F}_{\text{MTD}}(M, m)$ as the estimator obtained by applying \widehat{F} to the subsampled sequence $\{Z_{km}\}_{k=1}^{M'}$, where $m \in \mathbb{N}$ denotes the spacing between selected patches and $M' = \lfloor M/m \rfloor$ ensures the correct index range. Likewise, recall the definition from Definition 2.1 of $\widehat{F}_{\text{MRA}}(M)$ as the same function applied to M i.i.d. observations $\{Y_k\}_{k=1}^M$ drawn from the stationary distribution associated with the Markovian model.

Our objective is to compare the MSE of the Markovian estimator $\widehat{F}_{\text{MTD}}(M, m)$ to that of the i.i.d. estimator $\widehat{F}_{\text{MRA}}(M)$ in the asymptotic regime where $M \rightarrow \infty$. To make this comparison precise, we now formalize the notion of a convergence rate for the estimator $\widehat{F}(\cdot)$ in the i.i.d. MRA setting. This provides a rigorous characterization of how the estimation error decays as a function of the sample size and noise level.

Definition 4.1 (Convergence rate). *Let $M \in \mathbb{N}$, and let $\{Y_k\}_{k=1}^M$ be i.i.d. observations of the form (14), corresponding to i.i.d. samples $\{\tilde{g}_k\}_{k=1}^M$ drawn from a distribution π over a compact group G , corrupted by i.i.d. Gaussian noise $\{\varepsilon_k\}_{k=1}^M$ with variance σ^2 and zero mean. Let \widehat{F} be an estimator as defined in (7), mapping observations to an estimate of the features $\mathcal{F}(X) \in \mathbb{R}^d$. Define the i.i.d. estimator as $\widehat{F}_{\text{MRA}}(M) := \widehat{F}(\{Y_k\}_{k=1}^M)$. Given a function $a : (0, \infty) \rightarrow (0, \infty)$, we say that*

$\widehat{F}_{\text{MRA}}(M)$ has convergence rate $a(\sigma)$ if

$$\frac{\mathbb{E} \left[\left\| \widehat{F}_{\text{MRA}}(M) - \mathcal{F}(X) \right\|^2 \right]}{a(\sigma)/M} \xrightarrow[M \rightarrow \infty]{} 1.$$

Recall that following [2], the convergence rate $a(\sigma)$ is typically a polynomial function of the noise level σ , and is given by $a(\sigma) = \sigma^{2n_{\min}}$, where n_{\min} is the order of the lowest moment that determines the orbit of the signal under the group action.

4.1. Convergence to the IID MRA model. We are now in a position to present the main theorem of the 1D MTD model (proved in Appendix A.3), which establishes the sample complexity relationship between MTD patches and the associated MRA model with i.i.d. observations.

Theorem 4.2 (Convergence to MRA model). *Let the assumptions of Theorem 3.4 hold. Consider two observation models:*

- (i) *Let $\{Z_k\}_{k=1}^M$ denote the sequence of patches extracted from the MTD measurement Z as in (9), which, by Theorem 3.4, satisfy the Markovian MRA model (14) with group elements $\{g_k\}_{k=1}^M$ forming a Markov chain over a compact group G .*
- (ii) *Let $\{Y_k\}_{k=1}^M$ be i.i.d. samples of the form (14), with group elements $\{\tilde{g}_k\}_{k=1}^M$ drawn i.i.d. from the stationary distribution π associated to the Markov chain in Theorem 3.4.*

Let $\mathcal{F} : \mathbb{R}^L \rightarrow \mathbb{R}^d$ be a bounded continuous feature map, and let $\widehat{F} : \bigcup_{M \geq 1} (\mathbb{R}^L)^M \rightarrow \mathbb{R}^d$ be a bounded continuous estimator map such that the estimation associated to i.i.d. measurements, denoted by $\widehat{F}_{\text{MRA}}(M) := \widehat{F} \left[\{Y_k\}_{k=1}^M \right]$ has convergence rate $a(\sigma)$ as per Definition 4.1, for some function $a : (0, \infty) \rightarrow (0, \infty)$. Then the following statements hold:

- (i) *There exists $c_0 > 0$ such that, for any $m = \lfloor c \log(M) \rfloor$ with $c > c_0$, and taking $M' = \lfloor M/m \rfloor$, we have*

$$\frac{\mathbb{E} \left[\left\| \widehat{F} \left[\{Z_{km}\}_{k=1}^{M'} \right] - \mathcal{F}(X) \right\|^2 \right]}{a(\sigma)/M'} \rightarrow 1, \quad \text{as } M' \rightarrow \infty.$$

In particular, since $M' \sim \frac{M}{c \log(M)}$, the sample complexity in the MTD model matches that of the i.i.d. MRA model up to a logarithmic factor.

- (ii) *Suppose the estimator is of the form*

$$\widehat{F} \left[\{Y_k\}_{k=1}^M \right] = \frac{1}{M} \sum_{k=1}^M F(Y_k),$$

for some bounded continuous function $F : \mathbb{R}^L \rightarrow \mathbb{R}^d$, and assume $a(\sigma) \geq \tau$ for some constant $\tau > 0$. Then,

$$\limsup_{M \rightarrow \infty} \frac{\mathbb{E} \left[\left\| \widehat{F} \left[\{Z_k\}_{k=1}^M \right] - \mathcal{F}(X) \right\|^2 \right]}{a(\sigma)/M} \leq K,$$

where K is a constant depending on the mixing rate from Theorem 3.4 (i.e., on λ and L), the norm $\|F\|_\infty$, the lower bound τ , and the dimension of X .

Theorem 4.2 establishes that statistical estimation from the dependent MTD model (Markovian MRA) is asymptotically equivalent to estimation under the i.i.d. MRA model, up to a (possibly) logarithmic overhead. The result covers two regimes, distinguished by the structure of the estimator:

- (i) *General estimators via subsampling:* In the general case where \widehat{F} is not necessarily an empirical average, statistical guarantees can still be obtained by subsampling the MTD patches at logarithmic intervals. Specifically, selecting every $m = \lfloor c \log M \rfloor$ -th patch ensures sufficient decorrelation due to the exponential mixing of the underlying Markov chain. The resulting subsampled sequence of size $M' \asymp M/\log M$ behaves approximately as an i.i.d. sample, allowing the estimator to achieve the same convergence rate (up to constants) as in the i.i.d. MRA model. This approach requires only boundedness and mixing, without structural assumptions on \widehat{F} .
- (ii) *Empirical average estimators without subsampling:* When the estimator is an empirical mean $\widehat{F}(Z_k) = \frac{1}{M} \sum F(Z_k)$, one can retain all M patches without subsampling. This result implies that empirical average estimators can fully exploit the dependent data, achieving the same sample complexity (up to a constant factor) as if the observations were independent.

The distinction between the two regimes is one of *efficiency*. For general estimators, subsampling at logarithmic intervals is necessary for our theorem to apply: without subsampling, we cannot guarantee the desired statistical behavior, even though the estimator itself is well-defined. This restriction means that only a fraction $\sim 1/\log M$ of the available data is effectively used. By contrast, empirical average estimators can leverage all M patches without any loss, achieving the same sample complexity as in the i.i.d. setting. Consequently, Theorem 4.2(ii) provides strictly stronger guarantees whenever such estimators are applicable.

We emphasize that the convergence rate is defined relative to the stationary distribution of the group elements g_k in the MTD model. In the one-dimensional case, this stationary distribution is analytically characterized in terms of the density parameter λ and the patch length L (see Theorem 3.4). In higher dimensions, the spatial interactions are governed by more complex models, such as the hard-core process in 2D that we propose in sections 5 and 6, and understanding the induced distribution becomes substantially more involved. Nevertheless, the general equivalence principle established in Theorem 4.2 ensures that, under exponential mixing conditions, estimators that achieve a given statistical accuracy in the i.i.d. model will exhibit the same asymptotic rate when applied to MTD data, even in the presence of these dependencies.

4.2. Implication to the method of moments and the MTD sample complexity. A central application of Theorem 4.2(ii) is for the method of moments, as described in Section 2.1. Recall that in the i.i.d. setting, the n -th order moment of the random variable $Y \in \mathbb{R}^L$ defined in (3), is defined by (5). This moment can be empirically estimated using M i.i.d. observations $\{Y_k\}_{k=1}^M$ via:

$$(17) \quad \widehat{M}_{\text{MRA}}^n(\{Y_k\}_{k=1}^M) := \frac{1}{M} \sum_{k=1}^M (Y_k)^{\otimes n}.$$

Similarly, we define the n -th order empirical moment computed from the M patches $\{Z_k\}_{k=1}^M$ extracted from the MTD observation Z (similarly to Theorem 4.2(ii)), as follows:

$$(18) \quad \widehat{M}_{\text{MTD}}^n(\{Z_k\}_{k=1}^M) := \frac{1}{M} \sum_{k=1}^M (Z_k)^{\otimes n}.$$

We now formalize the consequence of Theorem 4.2(ii) for the method of moments.

Corollary 4.3 (Method of moments for MTD). *Let $n \in \mathbb{N}$, and denote by $M_{\text{MRA}}^n = \mathbb{E}[Y^{\otimes n}]$ the n -th order moment of the i.i.d. MRA model, where Y is as defined in (3). Let $\widehat{M}_{\text{MTD}}^n$ be the empirical n -th order moment computed from M consecutive patches $\{Z_k\}_{k=1}^M$ extracted from the MTD model, as defined in (18). Assume that the conditions of Theorem 4.2(ii) hold, and that the moment map $(\cdot)^{\otimes n} : \mathbb{R}^L \rightarrow \mathbb{R}^{L^{\otimes n}}$ is bounded on the support of the observations.*

Then:

(i) *There exists a constant $C > 0$ such that*

$$\limsup_{M \rightarrow \infty} \frac{\mathbb{E} \left[\left\| \widehat{M}_{\text{MTD}}^n(\{Z_k\}_{k=1}^M) - M_{\text{MRA}}^n \right\|^2 \right]}{a(\sigma)/M} \leq C,$$

where $a(\sigma)$ is the convergence rate from Definition 4.1, and C depends on n , $\|(M_{\text{MRA}}^n)^{\otimes n}\|_\infty$, and the mixing properties of the underlying Markov chain.

(ii) *Furthermore, suppose that n_{\min} is the minimal moment order required for orbit recovery in the i.i.d. MRA model (14), in the sense that the orbit of \overline{X} under the group action is uniquely determined by $\{M_{\text{MRA}}^n\}_{n=0}^{n_{\min}}$. Then, in the low-SNR regime $\sigma^2 \rightarrow \infty$, the sample complexity of the method of moments applied to MTD data satisfies:*

$$M = \omega(\sigma^{2n_{\min}}),$$

matching the asymptotic sample complexity of the corresponding i.i.d. MRA model up to constants.

Corollary 4.3 shows that the method of moments retains its asymptotic optimality when applied to dependent MTD data. Specifically, the empirical moment estimator $\widehat{M}_{\text{MTD}}^n$ converges to the true i.i.d. moment $M_{\text{MRA}}^n = \mathbb{E}[Y^{\otimes n}]$ with the same convergence rate as in the i.i.d. MRA model. This follows directly from Theorem 4.2(ii), which guarantees that empirical average estimators behave similarly under Markovian and i.i.d. sampling. The practical consequence is significant: for signals identifiable from moments up to order n , it suffices to estimate those n moments using the MTD data. Thus, the method of moments applied to the MTD patches achieves the same sample complexity scaling as in the i.i.d. model, namely, $M = \omega(\sigma^{2n_{\min}})$ in the low-SNR regime. We stress that in this section we focus on the number of samples required to recover the moments from empirical data. Previous results (see [2, 14, 9]) show how to recover the signal X itself from sufficiently accurate estimators of the moments, and therefore our sample complexity results apply to estimation of X itself by plugin.

5. THE TWO-DIMENSIONAL MTD MODEL: PRELIMINARIES

In the two-dimensional MTD model, the observation is a large noisy image containing multiple copies of $X \in \mathbb{R}^{L \times L}$ (Figure 2(a)). A key step in extending the MTD framework to two dimensions is to specify the placement model for these signal occurrences. Our requirements are twofold: (i) copies of X must not overlap, and (ii) sufficiently distant regions should behave nearly independently, so that local statistics do not induce long-range correlations. Among the various models that satisfy these conditions, the *hard-core model* provides a natural and parsimonious choice. It enforces only the exclusion constraint, that is preventing overlap, while otherwise leaving placements unconstrained. This minimal assumption guarantees that the induced random field exhibits strong mixing, with correlations between distant patches decaying rapidly, thereby allowing us to treat well-separated patches as nearly independent. Such exponential mixing is the structural property required for our sample-complexity analysis.

Originating in statistical physics, the hard-core model describes systems of finite-size, non-interpenetrating objects, where any configuration placing two objects closer than a prescribed exclusion distance has zero probability. This abstraction has broad relevance across domains, including: (i) finite-size particles in statistical mechanics [26], (ii) non-overlapping targets in imaging [32, 4], and (iii) exclusion processes in networks and ecology [25, 40]; see also [23, 39]. While alternative spatial processes, such as Markov random fields or interacting particle systems, can also exhibit mixing, the hard-core model remains analytically tractable, conceptually simple, and widely studied.

5.1. Model formulation. Let $X \in \mathbb{R}^{L \times L}$ be the target image and let $Z \in \mathbb{R}^{LM \times LM}$ be the observed image. We model Z as

$$(19) \quad Z = \sum_{i=1}^q (S(t_i) * X) + \varepsilon,$$

where $\varepsilon \in \mathbb{R}^{LM \times LM}$ has i.i.d. $\mathcal{N}(0, \sigma^2)$ entries and $q \in \mathbb{N}$ is the number of appearances of X . The placement parameters t_i take values in $\{0, 1, \dots, L(M-1)\}^2$, so that an $L \times L$ copy of X placed at t_i lies entirely within the image. For $t \in \{0, \dots, LM-1\}^2$, the indicator image (Kronecker delta at t), $S(t) \in \{0, 1\}^{LM \times LM}$ is defined by $S(t)[\xi] = \mathbf{1}\{\xi = t\}$ for $\xi \in \{0, \dots, LM-1\}^2$, and the convolution in (19) implements a zero-padded placement (no wrap-around):

$$(20) \quad (S(t) * X)[\xi_1, \xi_2] = \begin{cases} X[(\xi_1, \xi_2) - t], & \text{if } (\xi_1, \xi_2) - t \in \{0, \dots, L-1\}^2, \\ 0, & \text{otherwise.} \end{cases}$$

Thus, each t_i specifies the top-left anchor pixel of a copy of X inserted into Z .

5.2. Hard-core model. The hard-core model consists of three components: (i) a graph $\mathcal{G}_M = (V_M, E_M)$, whose vertices V_M represent potential placement sites for signal occurrences (i.e., the locations $\{t_i\}_{i=1}^q$) and whose edges E_M encode conflicts (i.e., pairs of sites that cannot be simultaneously occupied); (ii) a collection of *admissible configurations*, defined as subsets of V_M that respect the non-overlap constraint; and (iii) a probability measure over admissible configurations, parameterized by an activity $\lambda > 0$ that controls the expected density of occupied sites. In other

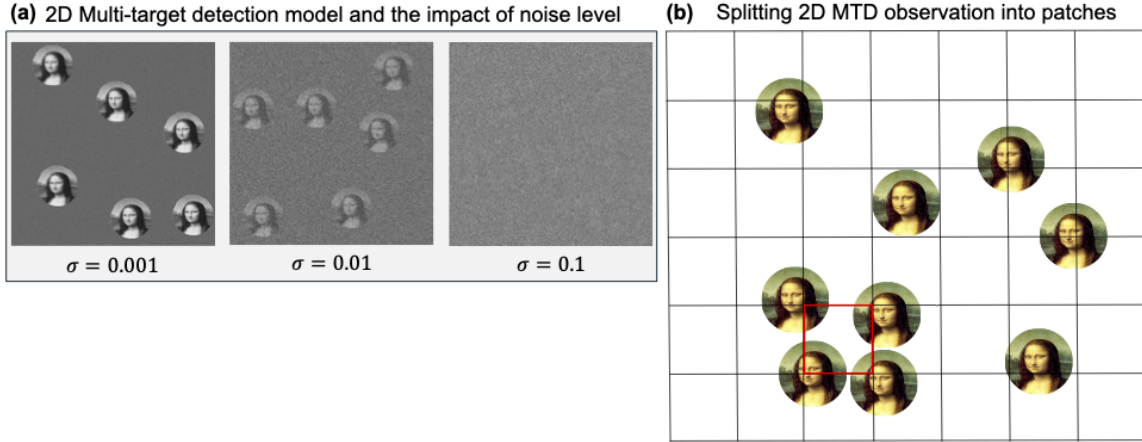


FIGURE 2. The MTD model in the 2D setting. (a) The 2D MTD model consists of multiple instances of an image (e.g., the Mona Lisa image) embedded at random locations within a noisy 2D observation. In the low-noise (high-SNR) regime, these instances can be reliably detected and localized. However, in the high-noise regime, the signal becomes indistinguishable from the background, making accurate localization infeasible. (b) To overcome this challenge, the observation is partitioned into non-overlapping patches. These patches form a structured variant of the MRA model, where neighboring patches exhibit statistical dependencies. We model these dependencies using a hard-core interaction, ensuring that overlapping signal occurrences are avoided. Each patch may intersect up to four distinct signal instances at its corners (appearing cropped in the patch), as illustrated in the red square.

words, in our setting, the placement parameters $\{t_i\}_{i=1}^q$ in (19) are modeled by a hard-core process ensuring that no two signal copies overlap.

In our setting, the vertices of the graph are given by

$$V_M = \{0, 1, \dots, L(M-1)\}^2,$$

corresponding to all possible anchor positions of $L \times L$ signal copies within the image. The edges are defined as

$$(t_1, t_2) \in E_M \iff \|t_1 - t_2\|_\infty \leq L-1,$$

where, for $t_i = (t_i^{(1)}, t_i^{(2)})$, we set

$$\|t_1 - t_2\|_\infty = \max(|t_1^{(1)} - t_2^{(1)}|, |t_1^{(2)} - t_2^{(2)}|).$$

Thus, two vertices are adjacent whenever their associated $L \times L$ patches overlap.

A configuration is a subset $\eta \subseteq V_M$. It is *admissible* if no two occupied vertices are adjacent, i.e., if $(t_j, t_k) \notin E_M$ for all $j \neq k$. Equivalently, admissibility requires that any two occupied sites be separated by at least L pixels in either the horizontal or vertical direction, ensuring that no two copies of the signal overlap. We will formalize this property next.

Definition 5.1 (Admissible configuration). *A configuration $\eta = \{t_i\}_{i=1}^q \subseteq V_M$ is admissible if it spans no edges in \mathcal{G}_M , i.e.*

$$(21) \quad (t_j, t_k) \notin E_M, \quad \forall j \neq k.$$

Equivalently, if the placement parameters in the 2D MTD model $\eta = \{t_i\}_{i=1}^q \subseteq V_M$ denotes the occupied set, an admissible configuration requires

$$(22) \quad \|t_j - t_k\|_\infty \geq L, \quad \text{for all } j \neq k.$$

Finally, the hard-core process is defined as a probability measure supported only on admissible configurations. For $\lambda > 0$, the probability of observing $\eta \subseteq V_M$ is

$$(23) \quad \mu_\lambda(\eta) = \frac{1}{Z_\lambda} \mathbf{1}\{\eta \text{ admissible}\} \lambda^{|\eta|}, \quad Z_\lambda = \sum_{\tau \subseteq V_M} \mathbf{1}\{\tau \text{ admissible}\} \lambda^{|\tau|}.$$

Here, λ (the activity or fugacity parameter) controls the density of occupied sites: larger values favor denser configurations. In this formulation, all admissible subsets of the same cardinality receive equal weight, proportional to $\lambda^{|\eta|}$, while inadmissible ones have probability zero. In our setting, the graph \mathcal{G}_M is chosen so that admissibility corresponds precisely to excluding overlapping $L \times L$ signal copies in the image. We next summarize this formally in Definition 5.2.

Definition 5.2 (The MTD hard-core model). *For $L \in \mathbb{N}$ fixed, and any $M \in \mathbb{N}$, let $\mathcal{G}_M = (V_M, E_M)$ be the MTD graph with set of vertices*

$$(24) \quad V_M := \{0, 1, \dots, L(M-1)\}^2,$$

and set of edges $E_M \subset V_M \times V_M$, such that for every $(x_1, y_1) \neq (x_2, y_2)$, the following is satisfied,

$$(25) \quad ((x_1, y_1), (x_2, y_2)) \in E_M \text{ whenever } \max\{|x_1 - x_2|, |y_1 - y_2|\} \leq L-1.$$

For any subset $\eta = \{t_i\}_{i=1}^q$ of V_M , we say that a vertex $v \in V_M$ is occupied whenever $v = t_i$ for some $i = 1, \dots, q$.

For any $\lambda > 0$, the hard-core model over the graph \mathcal{G}_M with parameter λ is a probability measure over the subsets of V_M , such that, for any $q \in \{0, \dots, |V_M|\}$, any subset $\eta = \{t_i\}_{i=1}^q$ with q elements has probability

$$\mu_\lambda(\eta) = \frac{1}{Z_\lambda} \lambda^q \mathbf{1}\{\eta \text{ is admissible}\},$$

where Z_λ is defined in (23), and the admissibility of η is given by the condition (21).

The admissibility condition (21) ensures the non-overlap of $L \times L$ signal footprints. Analogously to Assumption 3.1 in 1D, we assume signal placements $\{t_j\}_{j=1}^q$ are drawn from a hard-core model.

Assumption 5.3 (Hard-core model for distribution of placements). *There exists $\lambda > 0$ such that the placement parameters $\{t_i\}_{i=1}^q$ in (19) are distributed according to the hard-core model on \mathcal{G}_M with activity λ from Definition 5.2.*

At low activity λ , short-range repulsion yields weak long-range dependence and, under suitable conditions, exponential mixing [22, 23], which we formalize next.

5.3. Random fields and exponential mixing. The reduction of the 2D MTD problem to an MRA model follows the same idea as in the 1D case (see Section 3.3): we partition the measurement Z into non-overlapping patches Z_k . In two dimensions, it is convenient to index patches by their spatial location in the original image. For $M \in \mathbb{N}$, define

$$(26) \quad \mathcal{I}_M := \{1, \dots, M\}^2 = \{k = (k_1, k_2) : k_1, k_2 \in \{1, \dots, M\}\},$$

so that a total of M^2 disjoint $L \times L$ patches are extracted. Because the index set is two-dimensional, the collection $\{Z_k\}_{k \in \mathcal{I}_M}$ cannot be modeled as a hidden Markov process. Instead, we treat the group elements $\{g_k\}_{k \in \mathcal{I}_M}$ acting on the target signal as a *random field* on \mathcal{I}_M .

Definition 5.4 (Random field and admissibility). *Let G be a finite set and $\mathcal{I} \subset \mathbb{Z}^2$. A G -valued random field indexed by \mathcal{I} is a random variable $g = \{g_k\}_{k \in \mathcal{I}}$ which takes values in $G^\mathcal{I}$. For any index subset $S \subseteq \mathcal{I}$, we define the restriction of g to S as $g|_S = \{g_k\}_{k \in S}$, which takes values in G^S . We say that a configuration $\Psi \in G^S$ is admissible if $\mathbb{P}(g|_S = \Psi) > 0$.*

Definition 5.5 (Exponential mixing). *Let $\mathcal{I} \subset \mathbb{Z}^2$ be a two-dimensional index set, and define the complement of the index set as $\mathcal{I}^c := \mathbb{Z}^2 \setminus \mathcal{I}$. A G -valued random field $\{g_k\}_{k \in \mathcal{I}}$ satisfies exponential mixing if there exist $c_1, \gamma > 0$ and a probability distribution π on G such that for every $k \in \mathcal{I}$, $S \subseteq \mathcal{I}$, and admissible $\Psi \in G^S$,*

$$(27) \quad \max_{\varphi \in G} |\mathbb{P}(g_k = \varphi \mid g|_S = \Psi) - \pi(\varphi)| \leq c_1 \exp(-\gamma \cdot \text{dist}(k, S \cup \mathcal{I}^c)),$$

where, for $d(k, k') = \max_{j=1,2} |k_j - k'_j|$, we define $\text{dist}(k, A) = \min_{a \in A} d(k, a)$.

Intuitively, exponential mixing ensures that the statistical influence of distant sites decays exponentially, so well-separated patches behave nearly independently. The distance to the complement of the index set in the right hand side of (27) ensures that the statistical influence of the measurement boundary also decays exponentially as the patch is away from the edges of the image.

6. THE TWO-DIMENSIONAL MTD MODEL: MAIN RESULTS

Analogously to Section 3, we present the main results for the two-dimensional hard-core MTD model introduced in the previous section. In Section 6.1, we show that an MTD measurement can be partitioned into $L \times L$ patches, each of which has the form of a two-dimensional MRA observation (see Figure 2). Although these patches are not i.i.d., they are generated by an underlying random field that exhibits exponential mixing, governed by the distribution placement of the hard-core model (Assumption 5.3). In Section 6.2, we prove that this dependent MRA model converges to the classical i.i.d. MRA model; consequently, the sample complexity of the induced 2D hard-core model can be analyzed by comparison with the i.i.d. MRA framework.

6.1. From MTD to a non-i.i.d. MRA model with exponential mixing. As in the 1D case, we partition the measurement $Z \in \mathbb{R}^{LM \times LM}$ (see (19)) into M^2 non-overlapping $L \times L$ patches. Let $\mathcal{I}_M \triangleq \{1, \dots, M\}^2$ and, for $k = (k_1, k_2) \in \mathcal{I}_M$, define

$$(28) \quad Z_k[\xi] = Z[(k_1 - 1)L + \xi_1, (k_2 - 1)L + \xi_2], \quad \forall \xi = (\xi_1, \xi_2) \in \{0, \dots, L - 1\}^2.$$

Under Assumption 5.3 on the locations $\{t_i\}_{i=1}^q$ in (19) (which forbids overlap between signal occurrences), each patch $Z_k \in \mathbb{R}^{L \times L}$ can contain portions of at most four instances of the signal $X \in \mathbb{R}^{L \times L}$.

To model these contributions, we introduce the zero-padded signal

$$(29) \quad \tilde{X} \triangleq \begin{bmatrix} X & 0_{L \times L} \\ 0_{L \times L} & 0_{L \times L} \end{bmatrix} \in \mathbb{R}^{2L \times 2L},$$

and define the (componentwise) circular-shift action of $\mathbb{Z}_{2L} \times \mathbb{Z}_{2L}$ on $\mathbb{R}^{2L \times 2L}$ by

$$(30) \quad (\alpha, \beta) \cdot \tilde{X} [\xi_1, \xi_2] = \tilde{X} [(\xi_1 - \alpha, \xi_2 - \beta) \pmod{2L}], \quad \forall (\xi_1, \xi_2) \in \{0, \dots, 2L-1\}^2,$$

for any $(\alpha, \beta) \in \mathbb{Z}_{2L} \times \mathbb{Z}_{2L}$.

Since up to four shifted copies may contribute to a single patch (see Figure 2), set

$$(31) \quad \overline{X} \triangleq (\tilde{X}, \tilde{X}, \tilde{X}, \tilde{X}) \in (\mathbb{R}^{2L \times 2L})^4,$$

and let $G \triangleq (\mathbb{Z}_{2L} \times \mathbb{Z}_{2L})^4$ act componentwise on $(\mathbb{R}^{2L \times 2L})^4$:

$$(32) \quad g \cdot (\tilde{X}_0, \tilde{X}_1, \tilde{X}_2, \tilde{X}_3) = (g^{(1)} \cdot \tilde{X}_0, g^{(2)} \cdot \tilde{X}_1, g^{(3)} \cdot \tilde{X}_2, g^{(4)} \cdot \tilde{X}_3),$$

for $g = (g^{(1)}, g^{(2)}, g^{(3)}, g^{(4)}) \in G$.

Finally, define the linear operator $P : (\mathbb{R}^{2L \times 2L})^4 \rightarrow \mathbb{R}^{L \times L}$ by

$$(33) \quad P(\tilde{X}_0, \tilde{X}_1, \tilde{X}_2, \tilde{X}_3) = P_{00}\tilde{X}_0 + P_{01}\tilde{X}_1 + P_{10}\tilde{X}_2 + P_{11}\tilde{X}_3,$$

where $P_{00}, P_{01}, P_{10}, P_{11} : \mathbb{R}^{2L \times 2L} \rightarrow \mathbb{R}^{L \times L}$ extract, respectively, the top-left, top-right, bottom-left, and bottom-right $L \times L$ blocks. Namely, for

$$\tilde{X} = \begin{bmatrix} A & B \\ C & D \end{bmatrix}, \quad A, B, C, D \in \mathbb{R}^{L \times L},$$

we have $P_{00}\tilde{X} = A$, $P_{01}\tilde{X} = B$, $P_{10}\tilde{X} = C$, and $P_{11}\tilde{X} = D$.

We are now in a position to introduce the MRA model that describes the patches Z_k , defined in (28), extracted from the MTD measurement $Z \in \mathbb{R}^{LM \times LM}$ in (19).

Definition 6.1 (The induced hard-core two-dimensional MRA model). *Let $X \in \mathbb{R}^{L \times L}$ be the target signal, and let $\overline{X} \in (\mathbb{R}^{2L \times 2L})^4$ be given by (31). Let us consider the index set $\mathcal{I}_M := \{1, \dots, M\}^2$, and the finite abelian group $G := (\mathbb{Z}_{2L} \times \mathbb{Z}_{2L})^4$ acting on $(\mathbb{R}^{2L \times 2L})^4$ as described in (32). Let $P : (\mathbb{R}^{2L \times 2L})^4 \rightarrow \mathbb{R}^{L \times L}$ be the linear operator defined in (33). We consider the problem of recovering \overline{X} from noisy group-transformed and projected observations of \overline{X} with the form*

$$(34) \quad Z_k = P(g_k \cdot \overline{X}) + \varepsilon_k, \quad k \in \mathcal{I}_M,$$

where $\{g_k\}_{k \in \mathcal{I}_M}$ is a random field over G indexed by \mathcal{I}_M , and $\{\varepsilon_k\}_{k \in \mathcal{I}_M}$ is i.i.d. Gaussian noise.

The next result proves that the patch sequence Z_k defined in (28) admits the MRA representation of Definition 6.1, with latent group elements forming an exponentially mixing random field. The construction of this random field relies on the assumption that the placement of the signal occurrences $\{t_i\}_{i=1}^q$ is governed by a hard-core model on a 2D graph, where the vertices are the pixels of the image (Assumption 5.3). We refer to this model as the hard-core MRA model. The proof is given in Appendix A.2.

Theorem 6.2 (Induced MRA model with exponential mixing). *Let $L, M \in \mathbb{N}$ and let $X \in \mathbb{R}^{L \times L}$. Let the measurement $Z \in \mathbb{R}^{LM \times LM}$ be defined as in (19), with position parameters $\{t_i\}_{i=1}^q$ satisfying Assumption 5.3 for some $\lambda \in (0, 1)$. Suppose that Z is partitioned into non-overlapping patches $\{Z_k\}_{k \in \mathcal{I}_M}$ as in (28). Then, the patch sequence $\{Z_k\}_{k \in \mathcal{I}_M}$ can be expressed in the form (34), as in Definition 6.1, where $\{g_k\}_{k \in \mathcal{I}_M}$ is a random field over the group G . Moreover, there exists a constant $\lambda_0 \in (0, 1)$, depending only on L , such that if $\lambda \in (0, \lambda_0)$, then the random field $\{g_k\}_{k \in \mathcal{I}_M}$ satisfies the exponential mixing property (Definition 5.5) for some probability distribution π over G .*

In contrast to the one-dimensional Markov case (cf. (16)), the distribution π does not admit a simple closed form in 2D. Instead, it is constructed in the proof of Theorem 6.2 as follows:

- (i) *Local marginal and encoding.* In Step 2 of the proof of Theorem 6.2, in section A.2, we express the group elements $\{g_k\}_{k \in \mathcal{I}_M}$ associated to each patch as a function of the marginal of the hard-core process on a $2L \times 2L$ neighborhood of the corresponding patch.
- (ii) *Existence of a Gibbs measure in the infinite graph \mathbb{Z}^2 .* In Step 3 we prove that, by Corollary 2.6 of [39] (see also Lemma A.3 in section A.2), if λ is sufficiently small (with a threshold depending only on the graph connectivity, determined by L), the hard-core process on the finite graph \mathcal{G}_M (see Definition 5.2) satisfies a strong spatial mixing property, which implies the existence of a unique Gibbs measure μ on the infinite graph \mathbb{Z}^2 . The hard-core model can equivalently be expressed as the restriction of the Gibbs measure to the finite set of vertices V_M , conditionally on having no particles in the complement $\mathbb{Z}^2 \setminus V_M$.
- (iii) *Construction of π .* In Step 4, we combine the two previous points to construct the distribution π as a function of the marginal of the Gibbs measure μ in a $2L \times 2L$ finite graph. Let $V_0 \triangleq \{-L, \dots, L-1\}^2$ and let μ_0 be the marginal of μ on V_0 (so $|V_0| = (2L)^2$). The distribution π is defined as the pushforward of μ_0 under the encoding map $\Phi : \{0, 1\}^{V_0} \rightarrow G$, from (i), that associates each admissible configuration η with the corresponding group element in G .

Under this construction, we can prove that the random field $\{g_k\}_{k \in \mathcal{I}_M}$ satisfies the exponential mixing property in Definition 5.5 with respect to π .

6.2. Convergence to i.i.d. MRA and sample complexity. This section is the two-dimensional analogue of Section 4. We show that the induced 2D MRA model of Definition 6.1, obtained by extracting patches $\{Z_k\}_{k \in \mathcal{I}_M}$ from an MTD measurement Z , matches the standard i.i.d. MRA reconstruction problem with patches $\{Y_k\}_{k \in \mathcal{I}_M}$ of the form (34), where the group elements $\{\tilde{g}_k\}_{k \in \mathcal{I}_M}$ are i.i.d. from the distribution π specified in Theorem 6.2.

Analogously to the 1D setting, we reuse the feature map, estimators, and convergence-rate notion for the 2D model. Let $\mathcal{F} : \mathbb{R}^{L \times L} \rightarrow \mathbb{R}^d$ be the feature map from Section 2.2, adjusted to a domain of 2D images with size $L \times L$. For any estimator function \widehat{F} acting on collections of patches, define (analogously to Definition 2.1),

$$(35) \quad \widehat{F}_{\text{MRA}}(M) \triangleq \widehat{F}[\{Y_k\}_{k \in \mathcal{I}_M}], \quad \widehat{F}_{\text{MTD}}(M, m) \triangleq \widehat{F}[\{Z_{km}\}_{k \in \mathcal{I}_{\lfloor M/m \rfloor}}],$$

where $\{Y_k\}$ are MRA observations and $\{Z_k\}$ are 2D MTD patches sampled every m sites in each coordinate; both aim to estimate $\mathcal{F}(X)$. Due to the strong spatial mixing of the underlying hard-core model (see Lemma A.3) for the spatial placement of signal occurrences, subsampling with m large enough ensures enough decorrelation between the selected patches.

The convergence-rate notion mirrors the 1D case (see Definition 4.1) with the natural replacement of the sample size by the number of 2D patches, i.e., we say that $\widehat{F}_{\text{MRA}}(M)$ has convergence rate $a(\sigma)$ if

$$(36) \quad \frac{\mathbb{E}[\|\widehat{F}_{\text{MRA}}(M) - \mathcal{F}(X)\|^2]}{a(\sigma)/M^2} \xrightarrow[M \rightarrow \infty]{} 1.$$

The next theorem (proved in Appendix A.3) establishes the connection, in terms of MSE and sample complexity, between the induced MRA model from Theorem 6.2 and the associated i.i.d. MRA model.

Theorem 6.3 (Convergence to two-dimensional MRA model). *Under the assumptions of Theorem 6.2,*

- (i) *let $\{Z_k\}_{k \in \mathcal{I}_M}$ be the patches extracted from Z as in (28), which, by virtue of Theorem 6.2, can be written as in (34), with $\{g_k\}_{k \in \mathcal{I}_M}$ a random field over G satisfying the exponential mixing property from Definition 5.5;*
- (ii) *let $\{Y_k\}_{k \in \mathcal{I}_M}$ be measurements of the form (34), with $\{\tilde{g}_k\}_{k \in \mathcal{I}_M}$ i.i.d. from the probability distribution π over G from Theorem 6.2.*

Let $\mathcal{F} : \mathbb{R}^{L \times L} \rightarrow \mathbb{R}^d$ be a bounded continuous feature map, and let $\widehat{F}(\cdot)$ be a bounded continuous estimator map such that the estimator $\widehat{F}_{\text{MRA}}(M)$ defined in (35) has convergence rate $a(\sigma)$, i.e., (36) holds for some function $a : (0, \infty) \rightarrow (0, \infty)$. Then, the following statements hold:

- (i) *There exists $c_0 > 0$ such that, for any $m = \lfloor c \log(M) \rfloor$ with $c > c_0$, and taking $M' = \lfloor M/m \rfloor$, we have*

$$\frac{\mathbb{E} \left[\left\| \widehat{F} \left[\{Z_{km}\}_{k \in \mathcal{I}_{M'}} \right] - \mathcal{F}(X) \right\|^2 \right]}{a(\sigma)/(M')^2} \rightarrow 1, \quad \text{as } M' \rightarrow \infty.$$

In particular, since $(M')^2 \asymp \frac{M^2}{(c \log(M))^2}$, the sample complexity of dependent data matches the sample complexity in the i.i.d. case up to a logarithmic factor squared.

- (ii) *Suppose $\widehat{F}(\cdot)$ is of the form $\widehat{F}[\{Y_k\}_{k \in \mathcal{I}_M}] = \frac{1}{M^2} \sum_{k \in \mathcal{I}_M} F(Y_k)$ for some bounded continuous function $F : \mathbb{R}^{L \times L} \rightarrow \mathbb{R}^d$, and assume $a(\sigma) \geq \tau$ for some $\tau > 0$. Then,*

$$\limsup_{M \rightarrow \infty} \frac{\mathbb{E} \left[\left\| \widehat{F}[\{Z_k\}_{k \in \mathcal{I}_M}] - \mathcal{F}(X) \right\|^2 \right]}{a(\sigma)/M^2} \leq K,$$

for a constant K that depends only on $\lambda, L, \|F\|_\infty, \tau$ and the dimension of X .

Theorem 6.3 extends all one-dimensional results to the two-dimensional MTD setting. Under the hard-core process assumption, the $L \times L$ patches $\{Z_k\}_{k \in \mathcal{I}_M}$ admit the induced 2D MRA representation with latent group elements $\{g_k\}$ forming an exponentially-mixing random field. Consequently,

any estimator that attains MSE convergence rate $a(\sigma)$ in the i.i.d. 2D MRA model achieves the same rate on MTD data up to a squared logarithmic overhead arising from decorrelation: choosing a grid spacing $m \simeq C \log M$ in *each* coordinate yields an effective sample size $M'^2 \asymp M^2/(\log M)^2$, so the gap to i.i.d. is $(\log M)^2$.

As in 1D, statement (ii) in Theorem 6.3 shows that empirical-average estimators (when applicable) need no subsampling and thus exploit all M^2 patches. Their MSE continues to scale as $a(\sigma)/M^2$ under exponential mixing, matching the i.i.d. rate up to constants. The same implication holds for the method of moments: empirical n th-order moments computed from the 2D MTD patches converge to their i.i.d. counterparts at rate $a(\sigma)/M^2$. If n_{\min} is the minimal moment order needed for orbit recovery in the i.i.d. model, then in the low-SNR regime the required *number of patches* $N = M^2$ satisfies $N = \omega(\sigma^{2n_{\min}})$, identical scaling to the i.i.d. case.

7. DISCUSSION AND OUTLOOK

7.1. Sample complexity for the MTD model. In this work, we establish a formal connection between the MTD model and the classical i.i.d. MRA problem. In the one-dimensional setting, the MTD model is cast as a Markovian variant of MRA, while in two dimensions, it is cast as a hard-core interaction model. We show that the MSE in the Markovian or hard-core setting can be upper bounded by that of the corresponding i.i.d. MRA model. The resulting i.i.d. MRA model falls within the standard MRA paradigm, where the sample complexity is known to depend on the minimal moment that uniquely determines the orbit of the underlying signal. While this minimal moment has been explicitly characterized for several standard MRA models, determining it for the i.i.d. model induced by our Markovian construction remains an open problem. A resolution of this question would enable a sharper and fully explicit upper bound on the sample complexity of the MTD model.

7.2. MTD with an algebraic structure. A natural extension of the MTD model is to consider the case where the signal instances are related through an underlying algebraic structure. In this setting, referred to as the MTD model with algebraic structure, multiple transformed copies of a base signal are embedded at unknown locations within a long, noisy observation Z [12]. Specifically, let $g_i \in G$ be i.i.d. group elements sampled from a distribution ρ over a compact group G , and define $X_i = g_i \cdot X$, where the group action \cdot encodes the transformation applied to the signal. The observed signal is modeled as

$$(37) \quad Z = \sum_{i=0}^{N-1} S(t_i) * X_i + \varepsilon,$$

where $*$ denotes linear convolution, $S(t_i)$ are unknown location indicators determining the positions of each transformed signal copy, and $\varepsilon \sim \mathcal{N}(0, \sigma^2 I_{LM \times LM})$ represents additive Gaussian noise. As in the homogeneous case (see (1)), the goal is to estimate the signal based on the noisy superposition of its transformed instances. Due to the invariance of the statistical distribution of Z under the action of G , i.e., Z has the same distribution whether the underlying signal is X or $g \cdot X$ for any $g \in G$, the task reduces to recovering the G -orbit of X , namely the set $\{g \cdot X \mid g \in G\}$.

Adapting the current framework to this more general algebraic setting introduces several conceptual challenges. First, the model may involve continuous rather than discrete signals, necessitating a

reformulation of the Markov property and the hard-core interaction model in a continuous domain. Second, the composition of group actions under convolution does not necessarily yield a group structure, which complicates both modeling and analysis. One possible resolution is to restrict attention to a suitable subset of the product group, but this requires ensuring that the resulting structure remains compact.

7.3. Connection to cryo-EM and cryo-ET. A prominent example of the MTD model with algebraic structure arises in cryo-EM, which can be viewed as a specific instance of the model in (37) with the addition of a tomographic projection. In cryo-EM, the observed data $Z \in \mathbb{R}^{LM \times LM}$ consists of a 2D micrograph containing multiple occurrences of images $X_i \in \mathbb{R}^{L \times L}$, each given by

$$X_i = P(g_i \cdot X),$$

where X is the underlying 3D volume to be estimated, g_i are random elements of the three-dimensional special orthogonal group $G = \text{SO}(3)$, and P denotes a tomographic projection operator, which may also incorporate additional linear effects such as the microscope's point spread function and discretization. A key challenge in this setting is that the reduction technique developed in this work, from the dependent (e.g., Markovian or hard-core) model to an i.i.d. MRA model, applies only after the group action and projection have been applied. That is, the observed cropped instances take the form

$$P_2 \left(g_i^{(2)} \cdot P_1 \left(g_i^{(1)} \cdot X \right) \right),$$

where $g_i^{(1)}$ and $g_i^{(2)}$ are distinct group actions and P_1, P_2 are projection operators. This nested composition of group actions and projections does not naturally fit into the classical MRA framework, and thus falls outside the scope of the current analysis.

While extending our methodology to the cryo-EM setting poses challenges, primarily due to the complexities introduced by projection imaging, a more tractable and closely related direction arises in cryo-electron tomography (cryo-ET), particularly in the context of the *sub-tomogram averaging* problem. In this setting, projections are absent, and the observations more closely resemble the raw signal model studied in this work, making it a promising candidate for applying the techniques developed here.

ACKNOWLEDGMENTS

T.B. is supported by the BSF grant no. 2020159, by the NSF-BSF grant no. 2024791, and the ISF grant no. 1924/21. C.E.-Y. is supported by the Ramón y Cajal 2022 grant RYC2022-035966-I.

REFERENCES

- [1] E. Abbe, T. Bendory, W. Leeb, J. M. Pereira, N. Sharon, and A. Singer. Multireference alignment is easier with an aperiodic translation distribution. *IEEE Transactions on Information Theory*, 65(6):3565–3584, 2018.
- [2] E. Abbe, J. M. Pereira, and A. Singer. Estimation in the group action channel. In *2018 IEEE International Symposium on Information Theory (ISIT)*, pages 561–565. IEEE, 2018.
- [3] T. Amir, T. Bendory, N. Dym, and D. Edidin. The stability of generalized phase retrieval problem over compact groups. *arXiv preprint arXiv:2505.04190*, 2025.
- [4] A. Baddeley, E. Rubak, and R. Turner. *Spatial point patterns: methodology and applications with R*, volume 1. CRC press Boca Raton, 2016.

- [5] X.-C. Bai, G. McMullan, and S. H. Scheres. How cryo-EM is revolutionizing structural biology. *Trends in biochemical sciences*, 40(1):49–57, 2015.
- [6] A. Balanov, W. Huleihel, and T. Bendory. Expectation-maximization for multi-reference alignment: Two pitfalls and one remedy. *arXiv preprint arXiv:2505.21435*, 2025.
- [7] A. Balanov, S. Kreymer, and T. Bendory. A note on the sample complexity of multi-target detection. In *15th International Conference on Sampling Theory and Applications*.
- [8] A. Balanov, A. Zabatani, and T. Bendory. Structure from noise: Confirmation bias in particle picking in structural biology. *arXiv preprint arXiv:2507.03951*, 2025.
- [9] A. S. Bandeira, B. Blum-Smith, J. Kileel, J. Niles-Weed, A. Perry, and A. S. Wein. Estimation under group actions: recovering orbits from invariants. *Applied and Computational Harmonic Analysis*, 66:236–319, 2023.
- [10] A. S. Bandeira, M. Charikar, A. Singer, and A. Zhu. Multireference alignment using semidefinite programming. In *Proceedings of the 5th conference on Innovations in theoretical computer science*, pages 459–470, 2014.
- [11] T. Bendory, A. Bartesaghi, and A. Singer. Single-particle cryo-electron microscopy: Mathematical theory, computational challenges, and opportunities. *IEEE signal processing magazine*, 37(2):58–76, 2020.
- [12] T. Bendory, N. Boumal, W. Leeb, E. Levin, and A. Singer. Multi-target detection with application to cryo-electron microscopy. *Inverse Problems*, 35(10):104003, 2019.
- [13] T. Bendory, N. Boumal, W. Leeb, E. Levin, and A. Singer. Toward single particle reconstruction without particle picking: Breaking the detection limit. *SIAM Journal on Imaging Sciences*, 16(2):886–910, 2023.
- [14] T. Bendory, N. Boumal, C. Ma, Z. Zhao, and A. Singer. Bispectrum inversion with application to multireference alignment. *IEEE Transactions on signal processing*, 66(4):1037–1050, 2017.
- [15] T. Bendory, N. Dym, D. Edidin, and A. Suresh. A transversality theorem for semi-algebraic sets with application to signal recovery from the second moment and cryo-em. *Foundations of Computational Mathematics*, pages 1–28, 2025.
- [16] T. Bendory and D. Edidin. The sample complexity of sparse multireference alignment and single-particle cryo-electron microscopy. *SIAM Journal on Mathematics of Data Science*, 6(2):254–282, 2024.
- [17] T. Bendory, D. Edidin, W. Leeb, and N. Sharon. Dihedral multi-reference alignment. *IEEE Transactions on Information Theory*, 68(5):3489–3499, 2022.
- [18] O. Cappé, E. Moulines, and T. Rydén. *Inference in hidden Markov models*. Springer, 2005.
- [19] M. Chen, J. M. Bell, X. Shi, S. Y. Sun, Z. Wang, and S. J. Ludtke. A complete data processing workflow for cryo-ET and subtomogram averaging. *Nature methods*, 16(11):1161–1168, 2019.
- [20] Y. Cheng. Single-particle cryo-EM—how did it get here and where will it go. *Science*, 361(6405):876–880, 2018.
- [21] M. Dadon, W. Huleihel, and T. Bendory. Detection and recovery of hidden submatrices. *IEEE Transactions on Signal and Information Processing over Networks*, 10:69–82, 2024.
- [22] R. L. Dobrushin. The problem of uniqueness of a gibbsian random field and the problem of phase transitions. *Functional analysis and its applications*, 2(4):302–312, 1968.
- [23] H.-O. Georgii. *Gibbs measures and phase transitions*, volume 9 of *De Gruyter Studies in Mathematics*. Walter de Gruyter & Co., Berlin, second edition, 2011.
- [24] R. M. Glaeser. How good can cryo-EM become? *Nature methods*, 13(1):28–32, 2016.
- [25] M. Haenggi. *Stochastic geometry for wireless networks*. Cambridge University Press, 2013.
- [26] J.-P. Hansen and I. R. McDonald. *Theory of simple liquids: with applications to soft matter*. Academic press, 2013.
- [27] R. Henderson. The potential and limitations of neutrons, electrons and X-rays for atomic resolution microscopy of unstained biological molecules. *Quarterly reviews of biophysics*, 28(2):171–193, 1995.
- [28] R. Henderson. Avoiding the pitfalls of single particle cryo-electron microscopy: Einstein from noise. *Proceedings of the National Academy of Sciences*, 110(45):18037–18041, 2013.
- [29] S. Kreymer, A. Singer, and T. Bendory. A stochastic approximate expectation-maximization for structure determination directly from cryo-EM micrographs. *arXiv preprint arXiv:2303.02157*, 2023.
- [30] D. A. Levin and Y. Peres. *Markov chains and mixing times*, volume 107. American Mathematical Soc., 2017.
- [31] S. P. Meyn and R. L. Tweedie. *Markov chains and stochastic stability*. Springer Science & Business Media, 2012.
- [32] J. Moller and R. P. Waagepetersen. *Statistical inference and simulation for spatial point processes*. CRC press, 2003.
- [33] E. Nogales. The development of cryo-EM into a mainstream structural biology technique. *Nature methods*, 13(1):24–27, 2016.
- [34] J. S. Rosenthal. Convergence rates for Markov chains. *Siam Review*, 37(3):387–405, 1995.

- [35] M. Schaffer, S. Pfeffer, J. Mahamid, S. Kleindiek, T. Laugks, S. Albert, B. D. Engel, A. Rummel, A. J. Smith, W. Baumeister, et al. A cryo-FIB lift-out technique enables molecular-resolution cryo-ET within native *caenorhabditis elegans* tissue. *Nature methods*, 16(8):757–762, 2019.
- [36] A. Singer and F. J. Sigworth. Computational methods for single-particle electron cryomicroscopy. *Annual review of biomedical data science*, 3:163–190, 2020.
- [37] B. Toader, F. J. Sigworth, and R. R. Lederman. Methods for cryo-EM single particle reconstruction of macromolecules having continuous heterogeneity. *Journal of Molecular Biology*, 435(9):168020, 2023.
- [38] J. van den Berg. A constructive mixing condition for 2-d gibbs measures with random interactions. *The Annals of Probability*, 25(3):1316–1333, 1997.
- [39] D. Weitz. Counting independent sets up to the tree threshold. In *STOC’06: Proceedings of the 38th Annual ACM Symposium on Theory of Computing*, pages 140–149. ACM, New York, 2006.
- [40] T. Wiegand and K. A. Moloney. *Handbook of spatial point-pattern analysis in ecology*. CRC press, 2013.
- [41] P. Zhang. Advances in cryo-electron tomography and subtomogram averaging and classification. *Current opinion in structural biology*, 58:249–258, 2019.

APPENDIX A. PROOFS

A.1. Proof of Theorem 3.4. We prove the Theorem in three steps:

- (i) First we prove that every patch Z_k can be written as

$$Z_k = P(g_k \cdot \bar{X}) + \varepsilon_k$$

for some $g_k = (g_k^{(1)}, g_k^{(2)}) \in \mathbb{Z}_{2L} \times \mathbb{Z}_{2L}$ and $\varepsilon_k \in \mathbb{R}^L$. Recall that $\bar{X} = (\tilde{X}, \tilde{X})$, where $\tilde{X} = (X, 0_L)$.

- (ii) Then, we prove that Assumption 3.1 implies that the sequence $\{g_k\}_{k=1}^M$ is a Markov Chain over $\mathbb{Z}_{2L} \times \mathbb{Z}_{2L}$.
- (iii) Finally, we conclude the proof by proving that the aforementioned Markov Chain has a positive absolute spectral gap, and deduce explicitly the convergence estimate to the stationary probability distribution. The explicit expression for the stationary distribution is obtained in Lemma A.1.

Step 1: Since the patches $\{Z_k\}_{k=1}^M$ into which we divide the measurement Z have length L , any patch Z_k can contain, at most, two parts of the signal X (note that Assumption 3.1 implies that there cannot be two signals overlapping): one or both of a piece of X remaining from the previous patch Z_{k-1} , and a piece of a signal starting in the current patch Z_k .

Recalling the projection operator $P : \mathbb{R}^{2L} \times \mathbb{R}^{2L} \rightarrow \mathbb{R}^L$ from (13), and the group action of $\mathbb{Z}_{2L} \times \mathbb{Z}_{2L}$ on $\mathbb{R}^{2L} \times \mathbb{R}^{2L}$ defined in (12), we can write

$$P(g_k \cdot \bar{X}) = P(g_k^{(1)} \cdot \tilde{X}, g_k^{(2)} \cdot \tilde{X}) = P_0(g_k^{(1)} \cdot \tilde{X}) + P_1(g_k^{(2)} \cdot \tilde{X}).$$

Recall that P_0 is the linear operator that extracts the last L components of any vector in \mathbb{R}^{2L} , whereas P_1 extracts the first L components.

If Y_k contains the remainder of a signal which started in the previous patch, let’s say at the l -th pixel for some $l \in \{1, \dots, L-1\}$, then we set $g_k^{(1)} = l$, i.e. $g_k^{(1)} \cdot \tilde{X}$ is the signal \tilde{X} , shifted l pixels to the right. In this way, $P_0[g_k^{(1)} \cdot \tilde{X}]$ contains the remainder of the signal that started in

the previous patch. If, on the contrary, Z_k has no signal remaining from the previous patch, then we take $g_k^{(1)} = 0$. In this case, $P_0[g_k^{(1)} \cdot \tilde{X}] = P_0 \tilde{X} = 0_L$ is the vector of zeros.

If there is a new signal appearance starting in the patch Z_k , let's say at the l -th pixel for some $l \in \{0, \dots, L-1\}$, then we take $g_k^{(2)} = l$. In this way, $P_1[g_k^{(2)} \cdot \tilde{X}]$ contains the first part of the signal (the first $L-l$ pixels), which appears in the patch Z_k . In case there is no signal starting in the patch Z_k , we can take $g_k^{(2)} = L$, which yields $g_k^{(2)} \cdot \tilde{X} = [0_L, X]$, and therefore $P_1[g_k^{(2)} \cdot \tilde{X}] = 0_L$ is the vector of zeros.

Adding up the terms $P_0[g_k^{(1)} \cdot \tilde{X}]$ and $P_1[g_k^{(2)} \cdot \tilde{X}]$ along with the vector of i.i.d. Gaussian noise $\varepsilon_k \in \mathbb{R}^L$, we can represent all the possible configurations for a patch Z_k .

Step 2: The next step is to prove that the sequence $\{g_k\}_{k=1}^M = (g_k^{(1)}, g_k^{(2)})_{k=1}^M$ is a Markov Chain over $\mathbb{Z}_{2L} \times \mathbb{Z}_{2L}$.

Let $\{\omega_k\}_{k \geq 0}$ be the Markov Chain over $\{0, \dots, L\}$ such that the first term ω_0 is given by

$$(38) \quad \omega_0 = 0,$$

and the matrix of transition probabilities is

$$(39) \quad P = \begin{bmatrix} \lambda & (1-\lambda)\lambda & (1-\lambda)^2\lambda & \dots & (1-\lambda)^{L-1}\lambda & (1-\lambda)^L \\ 0 & \lambda & (1-\lambda)\lambda & \dots & (1-\lambda)^{L-2}\lambda & (1-\lambda)^{L-1} \\ \vdots & \vdots & \vdots & \ddots & \vdots & \vdots \\ 0 & 0 & 0 & \dots & \lambda & (1-\lambda) \\ \lambda & (1-\lambda)\lambda & (1-\lambda)^2\lambda & \dots & (1-\lambda)^{L-1}\lambda & (1-\lambda)^L \end{bmatrix}.$$

We shall prove that each random variable $(g_k^{(1)}, g_k^{(2)})$ in the sequence $\{(g_k^{(1)}, g_k^{(2)})\}_{k=1}^M$ can be written as a deterministic function of (ω_{k-1}, ω_k) , for each $k \in \{1, 2, \dots, M\}$, extracted from the Markov Chain $\{\omega_k\}_{k \geq 0}$.

Let us start with the first term of the sequence. Since Y_1 contains no remainder from previous patches, we have $g_1^{(1)} = 0$. By Assumption 3.1, for any $l \in \{0, \dots, L-1\}$, the probability of the first signal X appearance starting in the l -th pixel of the measurement is $(1-\lambda)^l\lambda$, and the probability of it starting in a pixel beyond the $(L-1)$ -th is $(1-\lambda)^L$. Therefore, $g_1^{(2)}$ is the random variable in $\{0, \dots, L\}$ with probabilities given by the first row in the matrix (39). Hence, we take

$$(40) \quad g_1 = (g_1^{(1)}, g_1^{(2)}) = (\omega_0, \omega_1),$$

i.e., g_1 is the random variable in $\mathbb{Z}_{2L} \times \mathbb{Z}_{2L}$ given by the first two terms of the Markov chain $\{\omega_k\}_{k \geq 0}$.

For the second patch, Y_2 , if $g_1^{(2)} = 0$ or $g_1^{(2)} = L$, then Y_2 contains no signal remainder from patch Y_1 , and then we take $g_2^{(1)} = 0$. In this case, $g_2^{(2)}$ follows the same distribution as $g_1^{(2)}$, which corresponds to the first or the last rows in the matrix P , depending on whether $g_1^{(2)} = 0$ or $g_1^{(2)} = L$. In case $0 < g_1^{(2)} < L$, we should take $g_2^{(1)} = g_1^{(2)} = \omega_1$, since $P_0[\omega_1 \cdot \tilde{X}]$ selects the second half of the shifted vector $\omega_1 \cdot \tilde{X}$. Concerning $g_2^{(2)}$, in view of Assumption 3.1, we need to take $g_2^{(2)} = \omega$, where ω follows a Geometric distribution starting from the first empty pixel after the signal remainder from

the previous patch. By the construction of the Markov Chain $\{\omega_k\}_{k \geq 1}$ (see the matrix of transition probabilities P in (39)), we can take $g_2^{(2)} = \omega_2$.

In general, applying a recurrent argument, for any $k \geq 2$, we can take

$$(41) \quad g_k^{(1)} = \begin{cases} \omega_{k-1} & \text{if } \omega_{k-1} \in \{0, \dots, L-1\} \\ 0 & \text{if } \omega_{k-1} = L, \end{cases} \quad \text{and} \quad g_k^{(2)} = \omega_k.$$

In this way, we have proved that, for any $k \geq 1$, the probability distribution $g_k = (g_k^{(1)}, g_k^{(2)})$ is given by a deterministic function of the random variables ω_k and ω_{k-1} . Hence, since $\{\omega_k\}_{k \geq 1}$ is a Markov Chain, so is $\{(g_k^{(1)}, g_k^{(2)})\}_{k \geq 1}$.

Step 3: Next, we prove that the Markov Chain $\{\omega_k\}_{k \geq 0}$ defined in (38)–(39) has a positive absolute spectral gap. For this, it is enough to verify that the Markov Chain is indecomposable and aperiodic (see [34, Section 4]). These two properties hold since, in view of the transition matrix P in (39), the state $\omega = L$ is accessible (with positive probability) from any other state, and from this state, the Markov Chain can transition (with positive probability) to any other state.

This argument proves the existence of a unique stationary distribution ρ on $\{0, \dots, L\}$, and that, if we call $\mu_k(\omega | \omega_m)$, with $m, k \geq 0$ the probability distribution of ω_{m+k} conditionally on ω_m , then the probability distribution $\mu_k(\cdot | \omega_m)$ converges to ρ as k tends to infinity. Using a coupling argument (see for instance [34, Section 6]) and the uniform minorization condition from [34, Section 6.2], we can obtain explicitly the following convergence estimate:

$$(42) \quad \|\mu_k(\cdot | \omega_m) - \rho\| = \frac{1}{2} \sum_{\omega=0}^L |\mu_k(\omega | \omega_m) - \rho(\omega)| \leq (1 - \beta)^k, \quad \text{for all } \omega_m \in \{0, \dots, L\},$$

where β is given in terms of the matrix of probability transition P in (39) by

$$\beta = \sum_{j=0}^L \min_i P_{ij} = (1 - \lambda)^{L-1} \lambda + (1 - \lambda)^L = (1 - \lambda)^{L-1}.$$

Using this convergence estimate for the Markov chain $\{\omega_k\}_{k \geq 1}$ and the choice of g_k in (40) and (41), we obtain in Lemma A.1 the stationary distribution associated to $\{g_k\}_{k \geq 1}$ and deduce the statement (iii) of the Theorem. \square

Lemma A.1. *Let $\{\omega_k\}_{k \geq 0} \subset \{0, 1, \dots, L\}$ be the Markov chain given by $\omega_0 = 0$ and the matrix of probability transitions (39), and let $\{g_k\}_{k \geq 1} = \{(g_k^{(1)}, g_k^{(2)})\}_{k \geq 1} \subset G = \mathbb{Z}_{2L} \times \mathbb{Z}_{2L}$ be given in terms of $\{\omega_k\}_{k \geq 1}$ by (40) and (41). Then $\{g_k\}_{k \geq 1}$ is a Markov chain over G and, for any $1 \leq k \leq m$ and $g' \in G$, there exists a constant $C > 0$, depending on λ and L , such that*

$$\sum_{g \in G} |\Pr(g_m = g | g_k = g') - \pi(g)| \leq C (1 - (1 - \lambda)^{L-1})^{m-k},$$

where π is the probability distribution over G given, for any $g = (x, y) \in G$, by

$$\pi(x, y) := \begin{cases} \frac{(1-\lambda)^L}{1+(L-1)\lambda} & \text{if } (x, y) = (0, L) \\ \frac{\lambda(1-\lambda)^{L-x}}{1+(L-1)\lambda} & \text{if } 1 \leq x < L \text{ and } y = L \\ \frac{\lambda(1-\lambda)^y}{1+(L-1)\lambda} & \text{if } x = 0 \text{ and } 0 \leq y < L \\ \frac{\lambda^2(1-\lambda)^{y-x}}{1+(L-1)\lambda} & \text{if } 1 \leq x \leq y < L \\ 0 & \text{else.} \end{cases}$$

Proof. Proving that $\{g_k\}_{k \geq 1}$ is a Markov chain over G was done in Step 2 of the proof of Theorem 3.4, using the choice of $g_k^{(1)}$ and $g_k^{(2)}$ in (40) and (41). Recall that each g_k depends only on (ω_k, ω_{k-1}) , and it is easy to prove that $(\omega_k, \omega_{k-1})_{k \geq 1}$ is a Markov chain over $\{0, 1, \dots, L\}^2$.

It is well known that the stationary distribution of the Markov chain $\{\omega_k\}_{k \geq 0}$, that we represent by the vector $\rho := (\rho(0), \dots, \rho(L)) \in [0, 1]^{L+1}$, is the normalized left-eigenvector of the matrix of transition probabilities associated to the eigenvalue 1. In this case, by solving the system of equations $\rho P = \rho$, with P given in (39), we obtain

$$(43) \quad \rho(x) := \begin{cases} \frac{\lambda}{1+(L-1)\lambda} & \text{for } x = 0, 1, \dots, L-1 \\ \frac{1-\lambda}{1+(L-1)\lambda} & \text{for } x = L. \end{cases}$$

Let us now define the probability distribution $\tilde{\rho}$ over $\{0, 1, \dots, L\}^2$ given by

$$(44) \quad \tilde{\rho}(\omega_k, \omega_{k-1}) = P(\omega_{k-1}, \omega_k) \rho(\omega_{k-1}), \quad \text{for each } (\omega_k, \omega_{k-1}) \in \{0, 1, \dots, L\}^2,$$

where $\rho(x)$ is given by (43), and $P(x, y)$ is given by the element in the position (x, y) in the matrix of probability transitions P defined in (39).

Using the properties of Markov chains, for any $m > k$, we obtain

$$\begin{aligned} \Pr [(\omega_m, \omega_{m-1}) | (\omega_k, \omega_{k-1})] &= \Pr [\omega_m | \omega_{m-1}, (\omega_k, \omega_{k-1})] \Pr [\omega_{m-1} | (\omega_k, \omega_{k-1})] \\ &= \Pr [\omega_m | \omega_{m-1}] \Pr [\omega_{m-1} | \omega_k], \\ &= P(\omega_{m-1}, \omega_m) \mu_{m-1-k}(\omega_{m-1} | \omega_k), \end{aligned}$$

for any $(\omega_m, \omega_{m-1}), (\omega_k, \omega_{k-1}) \in \{0, 1, \dots, L\}^2$. Here, we used the notation

$$\mu_{m-1-k}(\omega_{m-1} | \omega_k) = \Pr [\omega_{m-1} | \omega_k]$$

introduced in Step 3 of the proof of Theorem 3.4. Hence, combining this with the definition of $\tilde{\rho}$ in (44) and (42), we obtain the following convergence estimate for the Markov chain (ω_k, ω_{k-1}) :

$$\begin{aligned} & \frac{1}{2} \sum_{\omega_m, \omega_{m-1}} |\Pr[(\omega_m, \omega_{m-1}) | (\omega_k, \omega_{k-1})] - \tilde{\rho}(\omega_m, \omega_{m-1})| \\ &= \frac{1}{2} \sum_{\omega_m, \omega_{m-1}} P(\omega_{m-1}, \omega_m) |\mu_{m-1-k}(\omega_{m-1} | \omega_k) - \rho(\omega_{m-1})| \\ &\leq \frac{L+1}{2} (1-\beta)^{m-1-k}. \end{aligned}$$

Finally, using the construction of $g_k = (g_k^{(1)}, g_k^{(2)})$ in terms of (ω_k, ω_{k-1}) made in (40) and (41), we deduce the convergence result for the Markov chain $\{g_k\}_{k \geq 1}$ with π given by

$$\pi(g^{(1)}, g^{(2)}) = \begin{cases} \tilde{\rho}(g^{(2)}, g^{(1)}) & \text{if } (g^{(1)}, g^{(2)}) \in \{1, \dots, L-1\} \times \{0, \dots, L\} \\ \tilde{\rho}(g^{(2)}, 0) + \tilde{\rho}(g^{(2)}, L) & \text{if } g^{(1)} = 0 \text{ and } g^{(2)} \in \{0, \dots, L\} \\ 0 & \text{else.} \end{cases}$$

The final expression of π , given in the statement of the Lemma is obtained by replacing the values of ρ in (43) and the terms in the matrix P in (39) in the expression of $\tilde{\rho}$ in (44). \square

A.2. Proof of Theorem 6.2. In this proof, we use a similar structure to the one used in the proof of Theorem 3.4:

- (i) First we prove that for any $k \in \mathcal{I}_M := \{1, \dots, M\}^2$, the patch Z_k extracted from Z as in (28) can be written as

$$Z_k = P(g_k \cdot \bar{X}) + \varepsilon_k,$$

for some $g_k = (g_k^{(1)}, g_k^{(2)}, g_k^{(3)}, g_k^{(4)}) \in G = (\mathbb{Z}_{2L} \times \mathbb{Z}_{2L})^4$ and $\varepsilon_k \in \mathbb{R}^{L \times L}$. Recall the definition of $\bar{X} \in (\mathbb{R}^{2L \times 2L})^4$ in (31).

- (ii) Then, for each patch Z_k , we prove that the group element $g_k \in G$ associated to the k -th patch can be written in terms of the hard-core model from Assumption 5.3, restricted to a rectangular neighborhood of the patch, that we denote by $V_k \subset V_M$, where V_M are the vertices of the graph \mathcal{G}_M in Definition 5.2. This construction defines $\{g_k\}_{k \in \mathcal{I}_M}$ as a random field over G , indexed by \mathcal{I}_M .
- (iii) Using known results for the hard-core model we have that, for λ sufficiently small, the hard-core model from Assumption 5.3 satisfies a property known as strong spatial mixing. This property implies that, as the number of patches M^2 tends to infinity, the hard-core model converges to a unique Gibbs measure on the two-dimensional integer lattice \mathbb{Z}^2 . The strong spatial mixing also implies that, for patches Z_k far from the measurement boundary, the hard-core model restricted to V_k and the Gibbs measure restricted to V_k are exponentially close as probability measures.
- (iv) Since the Gibbs measure in \mathbb{Z}^2 is shift invariance, the restriction to any rectangle $V_k \subset V_M$ is the same for every $k \in \mathcal{I}_M$. Then, we use this restriction of the Gibbs measure to define, as in Step (ii), a probability distribution π over the group G . Using the strong spatial mixing from the previous step, we prove that the random field $\{g_k\}_{k \in \mathcal{I}_M}$ and the probability distribution π satisfy the exponential mixing property in Definition 5.5.

Remark A.2. Differently to the Markov chain $\{g_k\}_{k \geq 1}$ introduced in the proof of Theorem 3.4 for the 1D case, the two-dimensional random field $\{g_k\}_{k \in \mathcal{I}_M}$ constructed in this proof does not have a stationary distribution per se. However, for our convergence results in Theorems 4.2 and 6.3, we only need that

- (a) the probability distribution of g_k 's in patches Z_k which are far from the measurement boundary is exponentially close to a certain probability distribution π over G ;
- (b) the correlation between g_k 's associated to patches which are far apart from each other decays exponentially.

These two properties, which we together called exponential mixing in Definition 5.5, are satisfied by Markov chains with positive absolute spectral gap, taking π as the stationary distribution (note that the boundary of the index set $\{1, \dots, M\}$ in the 1D case is 0 and $M + 1$). In the 2D case, the random field $\{g_k\}_{k \in \mathcal{I}_M}$ and the probability distribution π constructed in this proof also satisfy these two properties, with the pushforward of the Gibbs measure on a given patch (which is stationary due to shift invariance) taking on the role of π .

Let us now proceed with the proof of Theorem 6.2.

Step 1: Let us recall the definition of the linear operator $P : (\mathbb{R}^{2L \times 2L})^4 \rightarrow \mathbb{R}^{L \times L}$ in (33), which is of the form

$$(45) \quad P(\tilde{X}_0, \tilde{X}_1, \tilde{X}_2, \tilde{X}_3) = P_{00}\tilde{X}_0 + P_{01}\tilde{X}_1 + P_{10}\tilde{X}_2 + P_{11}\tilde{X}_3,$$

for any $(\tilde{X}_0, \tilde{X}_1, \tilde{X}_2, \tilde{X}_3) \in (\mathbb{R}^{2L \times 2L})^4$.

Since the patches Z_k have size $L \times L$, in each of them there can be, at most, one pixel containing the pixel $X[0, 0]$ of the signal $X \in \mathbb{R}^{L \times L}$. In other words, for any $k = (k_1, k_2) \in \mathcal{I}_M$, there is at most one element in $\{t_i\}_{i=1}^q$ such that $t_i - kL \in \{0, \dots, L - 1\}^2$. Moreover, in view of the definition of Z_k in (28), the signal in Z_k might also contain a piece of X for which the pixel $X[0, 0]$ is contained in the patches Y_{k_1, k_2-1} , Y_{k_1-1, k_2} or Y_{k_1-1, k_2-1} .

Recall the group action of $\mathbb{Z}_{2L} \times \mathbb{Z}_{2L}$ on $\mathbb{R}^{2L \times 2L}$ defined in (30), which cyclically shifts the coordinates of $2L \times 2L$ matrices coordinate wise, and also the group action of $G = (\mathbb{Z}_{2L} \times \mathbb{Z}_{2L})^4$ on $(\mathbb{R}^{2L \times 2L})^4$, which applies the previous action component wise, as defined in (32). Next we choose, for each $k = (k_1, k_2) \in \mathcal{I}_M$, a group element $g_k = (g_k^{(1)}, g_k^{(2)}, g_k^{(3)}, g_k^{(4)}) \in G$ such that

- i) $P_{00} \left[g_k^{(1)} \cdot \tilde{X} \right]$ contains the part of X in Z_k for which the pixel $X[0, 0]$ is in the patch Z_k .
- ii) $P_{01} \left[g_k^{(2)} \cdot \tilde{X} \right]$ contains the part of X in Z_k for which the pixel $X[0, 0]$ is in the patch Y_{k_1, k_2-1} .
- iii) $P_{10} \left[g_k^{(3)} \cdot \tilde{X} \right]$ contains the part of X in Z_k for which the pixel $X[0, 0]$ is in the patch Y_{k_1-1, k_2} .
- iv) $P_{11} \left[g_k^{(4)} \cdot \tilde{X} \right]$ contains the part of X in Z_k for which the pixel $X[0, 0]$ is in the patch Y_{k_1-1, k_2-1} .

For each $k \in \mathcal{I}_M$, we define the parameter $\omega_k \in \{0, 1, \dots, L - 1\}^2 \cup \{(L, L)\}$, which takes a value in $\{0, 1, \dots, L - 1\}^2$ if the patch Z_k contains the pixel $X[0, 0]$ of some signal appearance X in Z , and

$\omega_k = (L, L)$ if Z_k does not contain the pixel $X[0, 0]$. More precisely, we define ω_k as

$$(46) \quad \omega_k := \begin{cases} t & \text{if } \{t_i - kL\}_{i=1}^q \cap \{0, \dots, L-1\}^2 = \{t\}, \\ (L, L) & \text{if } \{t_i - kL\}_{i=1}^q \cap \{0, \dots, L-1\}^2 = \emptyset. \end{cases}$$

Note that, due to the hard-core model assumption on $\{t_i\}_{i=1}^q$, the intersection $\{t_i - kL\}_{i=1}^q \cap \{0, \dots, L-1\}^2$ can contain, at most, one element.

Next we prove that, for any $k \in \mathcal{I}_M$, the group elements $g_k = (g_k^{(1)}, g_k^{(2)}, g_k^{(3)}, g_k^{(4)}) \in (\mathbb{Z}_{2L} \times \mathbb{Z}_{2L})^4$ can be chosen, respectively, in terms of the parameters

$$\omega_k, \quad \omega_{k_1, k_2-1}, \quad \omega_{k_1-1, k_2} \quad \text{and} \quad \omega_{k_1-1, k_2-1}, \quad \text{defined in (46).}$$

Of course, if $k = (k_1, k_2)$ is such that $k_1 = 0$ or $k_2 = 0$, the sub-indices in the above parameters may take negative values. In this case, the associated parameter ω is taken as $\omega = (L, L)$, or equivalently, we consider that patches Y_{k_1, k_2} with a negative sub-index are empty.

Let us recall the definition of \tilde{X} in (29), which is given by

$$\tilde{X} := \begin{bmatrix} X & 0_{L \times L} \\ 0_{L \times L} & 0_{L \times L} \end{bmatrix}.$$

If the parameter $\omega_k \in \{0, 1, \dots, L-1\}^2$, then the patch Z_k contains $X[0, 0]$ in its ω_k pixel. Therefore, the part of the signal X that appears in the patch Z_k is precisely $P_{00}[\omega_k \cdot \tilde{X}]$. If the patch Z_k does not contain the pixel $X[0, 0]$, then we can simply take $g_k^{(1)} = \omega_k = (L, L)$, so that $P_{00}[g_k^{(1)} \cdot \tilde{X}] = 0_{L \times L}$. In conclusion, for any $k \in \mathcal{I}_M$, we can take $g_k^{(1)} = \omega_k$.

If the parameter $\omega_{k_1, k_2-1} \in \{0, \dots, L-1\}^2$, then the patch Y_{k_1, k_2-1} contains $X[0, 0]$ in its ω_{k_1, k_2-1} pixel. Therefore, the remainder of this signal appearance in the patch Y_{k_1, k_2} is given by $P_{01}[\omega_{k_1, k_2-1} \cdot \tilde{X}]$. If the patch Y_{k_1, k_2-1} does not contain the pixel $X[0, 0]$, then we can again take $g_k^{(2)} = \omega_{k_1, k_2-1} = (L, L)$, so that $P_{01}[g_k^{(2)} \cdot \tilde{X}] = 0_{L \times L}$. Hence, we can take $g_k^{(2)} = \omega_{k_1, k_2-1}$.

By a similar reasoning, we can take $g_k^{(3)} = \omega_{k_1-1, k_2}$, which implies that $P_{10}[g_k^{(3)} \cdot \tilde{X}]$ contains the part of the signal X , appearing in Z_k , for which the pixel $X[0, 0]$ is contained in the patch Y_{k_1-1, k_2} ; and $P_{10}[g_k^{(3)} \cdot \tilde{X}] = 0_{L \times L}$ if the patch Y_{k_1-1, k_2} does not contain the pixel $X[0, 0]$, i.e. if $\omega_{k_1-1, k_2} = (L, L)$.

If the patch Y_{k_1-1, k_2-1} contains the pixel $X[0, 0]$, then $\omega_{k_1-1, k_2-1} \in \{0, 1, \dots, L-1\}^2$, and the remainder in Z_k of this signal appearance is given by $P_{11}[\omega_{k_1-1, k_2-1} \cdot \tilde{X}]$. If Y_{k_1-1, k_2-1} does not contain the pixel $X[0, 0]$, i.e., if $\omega_{k_1-1, k_2-1} = (L, L)$, then we can take $g_k^{(4)} = (0, 0)$.

In conclusion, for each $k \in \mathcal{I}_M$, the group element $g_k = (g_k^{(1)}, g_k^{(2)}, g_k^{(3)}, g_k^{(4)}) \in (\mathbb{Z}_{2L} \times \mathbb{Z}_{2L})^4$ can be taken as

$$(47) \quad g_k^{(1)} = \omega_k, \quad g_k^{(2)} = \omega_{k_1, k_2-1}, \quad g_k^{(3)} = \omega_{k_1-1, k_2}, \quad g_k^{(4)} = \begin{cases} \omega_{k-1} & \text{if } \omega_{k-1} \in \{0, \dots, L-1\}^2 \\ (0, 0) & \text{if } \omega_{k-1} = (L, L), \end{cases}$$

where the parameters ω_k are defined, in terms of $\{t_i\}_{i=1}^q$ by (46). In the definition of $g_k^{(4)}$ above, $k-1$ denotes (k_1-1, k_2-1) .

Step 2: Let us recall the graph $\mathcal{G}_M = (V_M, E_M)$, with vertices $V_M \subset \mathbb{Z}^2$ given by (24) and edges $E_M \subset V_M \times V_M$ defined in (25). Let us denote by Θ the random variable associated to the hard-core model on the graph \mathcal{G}_M with activity parameter $\lambda \in (0, 1)$; see Definition 5.2. The hard-core model Θ is a random variable that takes values in the independent subgraphs of the graph \mathcal{G}_M , i.e. subsets of V_M which contain no adjacent vertices. From now on, we represent subsets of V_M by means of a boolean matrix of the form $\eta = \{\eta_v : v \in V_M\} \in \{0, 1\}^{V_M}$. We recall that, for any $\eta \in \{0, 1\}^{V_M}$, we say that η is independent if and only if

$$\eta_v \eta_{v'} = 0 \quad \forall (v, v') \in E_M,$$

i.e. any two vertices v and v' which are connected by an edge, do not take the value 1 simultaneously. The probability function for the random variable Θ can therefore be written as

$$\mathbb{P}(\Theta = \eta) = \begin{cases} C^{-1} \lambda^{|\eta|} & \text{if } \eta \text{ is independent,} \\ 0 & \text{else,} \end{cases}$$

where, for each $\eta \in \{0, 1\}^{V_M}$, we write $|\eta| = \sum_{v \in V_M} \eta_v$ and C is the normalizing constant

$$C := \sum_{\substack{\eta \in \{0, 1\}^{V_M} \\ \text{indep.}}} \lambda^{|\eta|}.$$

In view of Assumption 5.3, the parameters $\{t_i\}_{i=1}^q$ in (19) can be written, in terms of the random variable, Θ as

$$\{t_i\}_{i=1}^q = \{v \in V_M : \Theta_v = 1\}.$$

By the definition of the parameter ω_k in (46) for each $k = (k_1, k_2) \in \mathcal{I}_M$, we can write ω_k in terms of the restriction of the hard-core model Θ to the rectangle

$$kL + \{0, \dots, L-1\}^2 = \{(Lk_1 + \xi_1, Lk_2 + \xi_2) : (\xi_1, \xi_2) \in \{0, \dots, L-1\}^2\}.$$

More precisely, we can write ω_k as

$$(48) \quad \omega_k := \{v \in kL + \{0, \dots, L-1\}^2 : \Theta_v = 1\},$$

with $\omega_k := (L, L)$ if $\Theta_v = 0$ for all $v \in kL + \{0, \dots, L-1\}$.

Also, in view of (47), for each $k = (k_1, k_2) \in \mathcal{I}_M$, the group element $g_k = (g_k^{(1)}, g_k^{(2)}, g_k^{(3)}, g_k^{(4)})$ can be written as a deterministic function of the parameters ω_k , ω_{k_1, k_2-1} , ω_{k_1-1, k_2} and ω_{k_1-1, k_2-1} . Hence, for any $k \in \mathcal{I}_M$, we can choose $g_k \in G$ uniquely in terms of the restriction of the hard-core model Θ to the rectangle $V_k \in \mathbb{Z}^2$ given by

$$(49) \quad V_k := kL + \{-L, \dots, L-1\}^2 = \{(Lk_1 + \xi_1, Lk_2 + \xi_2) : (\xi_1, \xi_2) \in \{-L, \dots, L-1\}^2\}.$$

For each $k \in \mathcal{I}_M$, let us denote by Θ_k the restriction of the random variable Θ to the rectangle V_k . Since the choice of $g_k \in G$ only depends on the random variable Θ_k , we can view $\{g_k\}_{k \in \mathcal{I}_M}$ as a random field over G , indexed by \mathcal{I}_M .

Step 3: Next, we claim that the hard-core model Θ on the graph $\mathcal{G}_M = (V_M, E_M)$ has a unique Gibbs measure on the infinite graph \mathbb{Z}^2 , with the same criterion for edge connectivity as in (25). This is a consequence of the following property, known as strong spatial mixing.

Lemma A.3 (Corollary 2.6 of [39]). *In a general hard-core model Θ , defined on a graph (V, E) , there exists a critical value $\lambda_c > 0$, depending on the maximal degree of the graph, such that for any $0 < \lambda < \lambda_c$ there exist constants c, γ depending on λ and the maximal degree such that for any vertex $v \in V$, any set of vertices $S_1 \subset V$, any $\tau \in \{0, 1\}$ and any configurations $\eta, \eta' \in \{0, 1\}^{S_1}$,*

$$(50) \quad |\mathbb{P}(\Theta_v = \tau \mid \Theta_{S_1} = \eta) - \mathbb{P}(\Theta_v = \tau \mid \Theta_{S_1} = \eta')| \leq c \exp(-\gamma \tilde{d}(v, \eta, \eta')),$$

where $\tilde{d}(v, \eta, \eta') = \min\{d(v, w) : \eta_w \neq \eta'_w\}$ is the smallest graph distance from v to a vertex (in S_1) on which η and η' differ.

Note that the sufficient condition on λ for strong spatial mixing to hold depends on the maximal degree of the graph, which in our case is $(2L + 1)^2$, due to the definition of the edges in (25), and since every vertex $v \in V_M$ is connected to all the vertices in the rectangle $v + \{-L, \dots, L\}^2$.

It is well known that strong spatial mixing implies the existence of a Gibbs measure μ defined on the infinite graph \mathbb{Z}^2 (see [23] and [38] for general theory on Gibbs measures, and [39] for the special case of hard-core models). The Gibbs measure μ is a probability distribution on the infinite-dimensional state space $\{0, 1\}^{\mathbb{Z}^2}$ and can be used to write the hard-core model on the finite graph $\mathcal{G}_M = (V_M, E_M)$, as the restriction of the Gibbs measure to V_M , conditionally on all the elements on the complement $V_M^c := \mathbb{Z}^2 \setminus V_M$ being 0. If we denote by $\bar{\Theta}$ the random variable on $\{0, 1\}^{\mathbb{Z}^2}$ associated to the Gibbs measure μ , then for any $\eta \in \{0, 1\}^{V_M}$, we can write the probability $\mathbb{P}[\Theta = \eta]$ as

$$\mathbb{P}[\Theta = \eta] = \mathbb{P}[\bar{\Theta} = \bar{\eta} \mid \bar{\Theta}_{V_M^c} = 0] = \frac{\mu(\bar{\eta})}{\mathbb{P}[\bar{\Theta}_{V_M^c} = 0]}, \quad \text{where } \mathbb{P}[\bar{\Theta}_{V_M^c} = 0] = \sum_{\substack{\tau \in \{0, 1\}^{\mathbb{Z}^2} \\ \tau_{V_M^c} = 0}} \mu(\tau).$$

Here, $\bar{\eta}$ is the extension by zeros of η from V_M to \mathbb{Z}^2 , i.e., $\bar{\eta}_v = \eta_v$ if $v \in V_M$ and $\bar{\eta}_v = 0$ if $v \in V_M^c$, and for any $\tau \in \{0, 1\}^{\mathbb{Z}^2}$, $\tau_{V_M^c}$ denotes the restriction of τ to the set $V_M^c = \mathbb{Z}^2 \setminus V_M$.

Step 4: In Step 2, we proved that the group element $g_k \in G$, for each $k \in \mathcal{I}_M$, is determined by restricting the hard-core model Θ on the graph \mathcal{G}_M , to the rectangle V_k defined in (49). The probability distribution π on G satisfying (27) will be constructed by restricting the Gibbs measure μ on \mathbb{Z}^2 , introduced in Step 3, to the rectangle V_k . Recall that the existence of this Gibbs measure is guaranteed by Lemma A.3, provided $\lambda \in (0, \lambda_0)$, where λ_0 is a constant depending only on L .

For each $k \in \mathcal{I}_M$, let us denote by μ_k the marginal of the Gibbs measure μ on the rectangle V_k defined in (49). Note that the support of μ_k is $\{0, 1\}^{V_k}$. Based on the construction of g_k in (47) and (48), which is in terms of the restriction of the hard-core model to the rectangle V_k , there is a probability distribution π_k on G associated to the measure μ_k . More precisely, π_k is the pushforward measure of μ_k under the encoding map from $\{0, 1\}^{V_k}$ to G constructed in (47) and (48). Due to the shift invariance of the Gibbs measure μ over \mathbb{Z}^2 , one can easily verify that all the marginals μ_k are equal, and hence, there exists a probability distribution π on G such that $\pi_k = \pi$ for all $k \in \mathcal{I}_M$.

Let us now prove that the random field $\{g_k\}_{k \in \mathcal{I}_M}$ and the probability distribution π satisfy (27). Let $k \in \mathcal{I}_M$, and let $S \subset \mathcal{I}_M$ be a subset of indices. Denoting V_k the rectangle defined in (49), let us define $V_S = \bigcup_{k' \in S} V_{k'}$. By the choice of g in (47), for any $\varphi \in G$, there is a unique associated configuration $\eta \in \{0, 1\}^{V_k}$ of the hard-core model Θ restricted to V_k , and for each admissible

configuration $\Psi \in G^{|S|}$, there is a unique admissible configuration $\tau \in \{0,1\}^{V_S}$ of the hard-core model Θ restricted to V_S . Then, we can write the probability of $g_k = \varphi$ and $g_S = \Psi$ in terms of the hard-core model Θ on $\mathcal{G}_M = (V_M, E_M)$ as

$$\mathbb{P}[g_k = \varphi] = \mathbb{P}[\Theta_{V_k} = \eta] \quad \text{and} \quad \mathbb{P}[g_S = \Psi] = \mathbb{P}[\Theta_{V_S} = \tau].$$

Using the relation between the hard-core model Θ and the random variable $\bar{\Theta}$ associated to the Gibbs measure μ on $\{0,1\}^{\mathbb{Z}^2}$, we can write

$$(51) \quad \mathbb{P}[g_k = \varphi] = \mathbb{P}[\bar{\Theta}_{V_k} = \eta \mid \bar{\Theta}_{V_M^c} = 0] \quad \text{and} \quad \mathbb{P}[g_S = \Psi] = \mathbb{P}[\bar{\Theta}_{V_S} = \tau \mid \bar{\Theta}_{V_M^c} = 0].$$

Let us now prove that

$$(52) \quad \mathbb{P}[g_k = \varphi \mid g_S = \Psi] = \mathbb{P}[\bar{\Theta}_{V_k} = \eta \mid (\bar{\Theta}_{V_S}, \bar{\Theta}_{V_M^c}) = (\tau, 0)].$$

We define the events $A := [g_k = \varphi]$, $B := [g_S = \Psi]$. The intersection of both events is given by $A \cap B = [(g_k, g_S) = (\varphi, \Psi)]$. Using the second identity in (51) and the formula of conditional probabilities, we can write $\mathbb{P}[B]$ as

$$\mathbb{P}[B] = \mathbb{P}[\bar{\Theta}_{V_S} = \tau \mid \bar{\Theta}_{V_M^c} = 0] = \frac{\mathbb{P}[(\bar{\Theta}_{V_S}, \bar{\Theta}_{V_M^c}) = (\tau, 0)]}{\mathbb{P}[\bar{\Theta}_{V_M^c} = 0]}$$

Similarly, the probability of the intersection $A \cap B$ is given by

$$\begin{aligned} \mathbb{P}[A \cap B] &= \mathbb{P}[(g_k, g_S) = (\varphi, \Psi)] = \mathbb{P}[(\bar{\Theta}_{V_k}, \bar{\Theta}_{V_S}) = (\eta, \tau) \mid \bar{\Theta}_{V_M^c} = 0] \\ &= \frac{\mathbb{P}[(\bar{\Theta}_{V_k}, \bar{\Theta}_{V_S}, \bar{\Theta}_{V_M^c}) = (\eta, \tau, 0)]}{\mathbb{P}[\bar{\Theta}_{V_M^c} = 0]}. \end{aligned}$$

Using the formula for the conditional probability, we have

$$\begin{aligned} \mathbb{P}[A \mid B] &= \frac{\mathbb{P}[A \cap B]}{\mathbb{P}[B]} = \frac{\mathbb{P}[(\bar{\Theta}_{V_k}, \bar{\Theta}_{V_S}, \bar{\Theta}_{V_M^c}) = (\eta, \tau, 0)]}{\mathbb{P}[(\bar{\Theta}_{V_S}, \bar{\Theta}_{V_M^c}) = (\tau, 0)]} \\ &= \mathbb{P}[\bar{\Theta}_{V_k} = \eta \mid (\bar{\Theta}_{V_S}, \bar{\Theta}_{V_M^c}) = (\tau, 0)], \end{aligned}$$

and (52) is proven.

On the other hand, using the law of total probability, we have

$$(53) \quad \pi(\varphi) = \mathbb{P}[\bar{\Theta}_{V_k} = \eta] = \sum_{\substack{\tau_1 \in \{0,1\}^{V_S} \\ \tau_2 \in \{0,1\}^{V_M^c}}} \mathbb{P}[\bar{\Theta}_{V_k} = \eta \mid (\bar{\Theta}_{V_S}, \bar{\Theta}_{V_M^c}) = (\tau_1, \tau_2)] \mathbb{P}[(\bar{\Theta}_{V_S}, \bar{\Theta}_{V_M^c}) = (\tau_1, \tau_2)].$$

Combining (52) and (53), with the strong spatial mixing property from Lemma A.3, we obtain

$$\begin{aligned} &|\mathbb{P}[g_k = \varphi \mid g_S = \Psi] - \pi(\varphi)| \leq \\ &\sum_{\substack{\tau_1 \in \{0,1\}^{V_S} \\ \tau_2 \in \{0,1\}^{V_M^c}}} \left| \mathbb{P}[\bar{\Theta}_{V_k} = \eta \mid \bar{\Theta}_{V_S, V_M^c} = (\tau, 0)] - \mathbb{P}[\bar{\Theta}_{V_k} = \eta \mid \bar{\Theta}_{V_S, V_M^c} = (\tau_1, \tau_2)] \right| \mathbb{P}[\bar{\Theta}_{V_S, V_M^c} = (\tau_1, \tau_2)] \\ &\leq c_0 \exp(-\gamma d(V_k, V_S \cup V_M^c)), \end{aligned}$$

where $d(V_k, V_S \cup V_M^c)$ denotes the distance between the sets V_k and $V_S \cup V_M^c$ in the 2-dimensional lattice \mathbb{Z}^2 . In view of the construction of the rectangles V_M in (24) and V_k in (49), we see that $d(k, S \cup \mathcal{I}_M^c) \leq Ld(V_k, V_S \cup V_M^c)$, and property (27) then follows with exponent γ/L . \square

A.3. Proof of Theorems 4.2 and 6.3. The proof is almost identical for both theorems, and relies on the mixing properties of the group elements g_k which appear in the induced MRA model for the patches Z_k . The main difference is the index set, which is $k \in \{1, \dots, M\}$ for the one-dimensional case (Theorem 4.2) and $k \in \{1, \dots, M\}^2$ in the two-dimensional case (Theorem 6.3). In both cases, we denote the index set by \mathcal{I}_M , and $|\mathcal{I}_M|$ denotes the cardinality of \mathcal{I}_M (i.e., $|\mathcal{I}_M| = M$ for the 1D case, and $|\mathcal{I}_M| = M^2$ for the 2D case).

Note that, in the 1D case, the Markov chain $\{g_k\}_{k=1}^M$ from Theorem 3.4 can be seen as a random field over G indexed by $\mathcal{I}_M = \{1, 2, \dots, M\} \subset \mathbb{Z}$; see Definition 5.4. Moreover, the Markovian property, together with property (15) proved in Theorem 3.4, imply the following mixing property: for any $k \in \mathcal{I}_M = \{1, 2, \dots, M\}$, any $S \subset \mathcal{I}_M$ with $s < k$ for all $s \in S$, and any admissible $\Psi \in G^S$,

$$(54) \quad |\mathbb{P}(g_k = \varphi \mid g_{|S} = \Psi) - \pi(\varphi)| \leq C \exp(-\gamma(k - s_0)),$$

where $s_0 = \max(S)$ or $s_0 = 0$ if $S = \emptyset$. Here, we take $\gamma = -\log(1 - (1 - \lambda)^{L-1}) > 0$ and $C > 0$ the same constant as in Theorem 3.4. The mixing property (54) can be seen as a one-dimensional version of the mixing property in Definition 5.5 noting that, in this case, the states $\{g_k\}_{k=1}^M$ have a natural ordering.

In view of Theorems 3.4 and 6.2, in both cases, the patches $\{Z_k\}_{k \in \mathcal{I}_M}$ extracted from the MTD measurement Z , can be written as

$$(55) \quad Z_k = P(g_k \cdot \bar{X}) + \varepsilon_k, \quad \text{for } k \in \mathcal{I}_M,$$

for some projection operator P and some group elements $\{g_k\}_{k \in \mathcal{I}_M}$ in G , acting on the target signal \bar{X} , and ε_k being i.i.d. Gaussian noise with variance $\sigma^2 > 0$. We also recall, from the statement of the theorem, the definition of the i.i.d. measurements $\{Y_k\}_{k \in \mathcal{I}_M}$, which have the same form of (55), but with group elements $\{\tilde{g}_k\}_{k \in \mathcal{I}_M}$ being i.i.d. from a suitable probability distribution π over G .

Part (i): Let $c > 0$ be a constant to be chosen later. For any $M \in \mathbb{N}$, choose $m = \lfloor c \log(M) \rfloor$ and $M' = \lfloor M/m \rfloor$. We define the index set

$$\mathcal{I}'_M := \{km, : k \in \mathcal{I}_{M'}\}.$$

The cardinality of the index set is $|\mathcal{I}'_M| = M'$ in the 1D case, and $|\mathcal{I}'_M| = (M')^2$ in the 2D case. Note that $\mathcal{I}'_M \subset \mathcal{I}_M$. Moreover, in the 1D case we have

$$(56) \quad k - k' \geq m = \lfloor c \log(M) \rfloor, \quad \forall k, k' \in \mathcal{I}'_M, \text{ with } k > k',$$

whereas in the 2D case we have

$$(57) \quad d(k, k') \geq m = \lfloor c \log(M) \rfloor, \quad \forall k, k' \in \mathcal{I}'_M,$$

$d(k, k') = \max_{j \in \{1, 2\}} |k_j - k'_j|$. Considering \mathcal{I}'_M as a subset of \mathcal{I}_M , we also have that $d(k, \mathcal{I}_M^c) > m$ for all $k \in \mathcal{I}'_M$, where $\mathcal{I}_M^c = \mathbb{Z}^j \setminus \mathcal{I}_M$, with $j = 1$ in the 1D case, and $j = 2$ in the 2D case.

We are therefore in position to apply the mixing property (54) in the 1D case, and (27) in the 2D case for any $k \in \mathcal{I}'_M$ with $S = \mathcal{I}'_M \setminus \{k\}$.

Let us denote by π_M the probability density function associated to the marginal of the random field $\{g_k\}_{k \in \mathcal{I}_M}$ to the subset of indices \mathcal{I}'_M , and let $\tilde{\pi}_M$ be the probability density function of the marginal of the random field $\{\tilde{g}_k\}_{k \in \mathcal{I}_M}$ to \mathcal{I}'_M . Note that the latter is an i.i.d. sampling from π , whereas the former is extracted from a random field satisfying the mixing property (54) and (27) respectively for the 1D and the 2D cases.

Now we choose, in the 2D case, an arbitrary ordering of the index set \mathcal{I}'_M , so that any $\Psi \in G^{\mathcal{I}'_M}$ can be written as an ordered list of the form $\Psi = (\psi_1, \psi_2, \dots, \psi_{|\mathcal{I}'_M|}) \in G^{|\mathcal{I}'_M|}$. In the 1D case, we choose the natural ordering of the index set $\mathcal{I}'_M := \{m, 2m, 3m, \dots, mM'\}$.

We claim that there exists $c_1 > 0$, independent of M' , such that the ℓ_1 distance between $\tilde{\pi}_M$ and π_M satisfies

$$(58) \quad \|\pi_M - \tilde{\pi}_M\|_1 := \sum_{\Psi} |\pi_M(\Psi) - \tilde{\pi}_M(\Psi)| \leq (M')^j |G| c_1 e^{-\gamma m},$$

for any $\Psi \in G^{|\mathcal{I}'_M|}$, and where $j = 1$ in the 1D case and $j = 2$ in the 2D case.

Using the notation $\Psi_{1:j}$ to denote the vector $(\psi_1, \dots, \psi_j) \in G^j$, define

$$A_j = \sum_{\Psi_{1:j}} |\mathbb{P}(g_{1:j} = \Psi_{1:j}) - \mathbb{P}(\tilde{g}_{1:j} = \Psi_{1:j})|,$$

so that $\|\tilde{\pi}_M - \pi_M\|_1 = A_{|\mathcal{I}'_M|}$. Due to the mixing properties¹, and the fact that $\mathbb{P}(\tilde{g}_1 = \Psi_1) = \pi(\Psi_1)$, we have that $A_1 \leq |G| c_1 e^{-\gamma m}$, where $|G|$ is the cardinality of the finite group G .

Now, using that

$$\mathbb{P}(g_{1:j} = \Psi_{1:j}) = \mathbb{P}(g_j = \Psi_j \mid g_{1:j-1} = \Psi_{1:j-1}) \mathbb{P}(g_{1:j-1} = \Psi_{1:j-1}),$$

and that

$$\mathbb{P}(\tilde{g}_{1:j} = \Psi_{1:j}) = \pi(\Psi_j) \mathbb{P}(\tilde{g}_{1:j-1} = \Psi_{1:j-1}),$$

for all j and $\Psi_{1:j}$, we can decompose

$$\begin{aligned} |\mathbb{P}(g_{1:j} = \Psi_{1:j}) - \mathbb{P}(\tilde{g}_{1:j} = \Psi_{1:j})| &\leq \mathbb{P}(g_{1:j-1} = \Psi_{1:j-1}) |\mathbb{P}(g_j = \Psi_j \mid g_{1:j-1} = \Psi_{1:j-1}) - \pi(\Psi_j)| \\ &\quad + \pi(\Psi_j) |\mathbb{P}(g_{1:j-1} = \Psi_{1:j-1}) - \mathbb{P}(\tilde{g}_{1:j-1} = \Psi_{1:j-1})| \end{aligned}$$

Hence, we obtain

$$\begin{aligned} A_j &\leq \sum_{\Psi_{1:j}} \mathbb{P}(g_{1:j-1} = \Psi_{1:j-1}) |\mathbb{P}(g_j = \Psi_j \mid g_{1:j-1} = \Psi_{1:j-1}) - \pi(\Psi_j)| \\ &\quad + \sum_{\Psi_{1:j}} \pi(\Psi_j) |\mathbb{P}(g_{1:j-1} = \Psi_{1:j-1}) - \mathbb{P}(\tilde{g}_{1:j-1} = \Psi_{1:j-1})| \\ &= I + II. \end{aligned}$$

Using again the mixing properties², we can estimate I as

$$I \leq c_1 e^{-\gamma m} \sum_{\Psi_{1:j}} \mathbb{P}(g_{1:j-1} = \Psi_{1:j-1}) = c_1 e^{-\gamma m} \sum_{\Psi_j} \underbrace{\sum_{\Psi_{1:j-1}} \mathbb{P}(g_{1:j-1} = \Psi_{1:j-1})}_{=1} = |G| c_1 e^{-\gamma m}.$$

For the term II , we can factor out $\pi(\Psi_j)$ to obtain

$$II = \underbrace{\sum_{\Psi_j} \pi(\Psi_j)}_{=1} \sum_{\Psi_{1:j-1}} |\mathbb{P}(g_{1:j-1} = \Psi_{1:j-1}) - \mathbb{P}(\tilde{g}_{1:j-1} = \Psi_{1:j-1})| = A_{j-1}.$$

¹(54) and (56) in the 1D case; and (27) and (57) in the 2D case.

²(54) and (56) in the 1D case; and (27) and (57) in the 2D case.

We therefore obtain $A_j \leq |G|c_1 e^{-\gamma m} + A_{j-1}$, and hence, $\|\pi_M - \tilde{\pi}_M\|_1 = A_{|\mathcal{I}'_M|} \leq |\mathcal{I}'_M| |G|c_1 e^{-\gamma m}$. Finally, since the cardinality of the index set $|\mathcal{I}'_M|$ is M' in the 1D case, and $(M')^2$ in the 2D case, the claim (58) follows.

Now, for any bounded estimator $\hat{F}(\cdot)$, and using the law of total expectation, we can write the MSE for the samples $\{Z_k\}_{k \in \mathcal{I}'_M}$ and $\{Y_k\}_{k \in \mathcal{I}'_M}$, respectively, as

$$\mathbb{E} \left[\left\| \hat{F}(\{Z_k\}_{k \in \mathcal{I}'_M}) - \mathcal{F}(X) \right\|^2 \right] = \sum_{\Psi} \mathbb{E} \left[\left\| \hat{F}(\{Z_k\}_{k \in \mathcal{I}'_M}) - \mathcal{F}(X) \right\|^2 \mid \{g_k\}_{k \in \mathcal{I}'_M} = \Psi \right] \pi_M(\Psi)$$

and

$$\mathbb{E} \left[\left\| \hat{F}(\{Y_k\}_{k \in \mathcal{I}'_M}) - \mathcal{F}(X) \right\|^2 \right] = \sum_{\Psi} \mathbb{E} \left[\left\| \hat{F}(\{Y_k\}_{k \in \mathcal{I}'_M}) - \mathcal{F}(X) \right\|^2 \mid \{\tilde{g}_k\}_{k \in \mathcal{I}'_M} = \Psi \right] \tilde{\pi}_M(\Psi).$$

Since the difference between $\{Z_k\}_{k \in \mathcal{I}'_M}$ and $\{Y_k\}_{k \in \mathcal{I}'_M}$ is only the probability distribution for the group elements $\{g_k\}_{k \in \mathcal{I}'_M}$, we have that the MSE, conditionally on $\{g_k\}_{k \in \mathcal{I}'_M}$, is the same for both cases. In other words, for any admissible $\Psi \in G^{\mathcal{I}'_M}$, we have

$$\mathbb{E} \left[\left\| \hat{F}(\{Z_k\}_{k \in \mathcal{I}'_M}) - \mathcal{F}(X) \right\|^2 \mid \{g_k\}_{k \in \mathcal{I}'_M} = \Psi \right] = \mathbb{E} \left[\left\| \hat{F}(\{Y_k\}_{k \in \mathcal{I}'_M}) - \mathcal{F}(X) \right\|^2 \mid \{\tilde{g}_k\}_{k \in \mathcal{I}'_M} = \Psi \right].$$

Hence, using the boundedness of $\hat{F}(\cdot)$ and the estimate (58), we deduce the existence of a constant $C > 0$, which is independent of M , such that

$$\begin{aligned} \left| \mathbb{E} \left[\left\| \hat{F}(\{Z_k\}_{k \in \mathcal{I}'_M}) - \mathcal{F}(X) \right\|^2 \right] - \mathbb{E} \left[\left\| \hat{F}(\{Y_k\}_{k \in \mathcal{I}'_M}) - \mathcal{F}(X) \right\|^2 \right] \right| &\leq C \sum_{\Psi} |\pi_M(\Psi) - \tilde{\pi}_M(\Psi)| \\ &\leq C |G| c_1 (M')^j e^{-\gamma m} \end{aligned}$$

Finally, for the convergence rate $a(\sigma)$ from (36), we can compute

$$\left| \frac{\mathbb{E} \left[\left\| \hat{F}(\{Z_k\}_{k \in \mathcal{I}'_M}) - \mathcal{F}(X) \right\|^2 \right]}{a(\sigma)/(M')^j} - 1 \right| \leq C |G| c_1 \frac{(M')^{2j}}{a(\sigma)} e^{-\gamma m} + \left| \frac{\mathbb{E} \left[\left\| \hat{F}(\{Y_k\}_{k \in \mathcal{I}'_M}) - \mathcal{F}(X) \right\|^2 \right]}{a(\sigma)/(M')^j} - 1 \right|.$$

Since we chose $m = \lfloor c \log M \rfloor$ and $M' = \lfloor M/m \rfloor$ for a constant c , we deduce that the first term in the right-hand side vanishes as $M' \rightarrow \infty$ (which implies $M \rightarrow \infty$) provided the constant c is large enough (we need $c \geq c_0 = 2/\gamma$ for the 1D case and $c \geq c_0 = 4/\gamma$ for the 2D case). The second term in the right-hand side of the above inequality also vanishes by assumption, since the estimator $\hat{F}(\cdot)$ has convergence rate $a(\sigma)$ for the i.i.d. measurements $\{Y_k\}_{k \in \mathcal{I}'_M}$ (see Definition 4.1). The first statement of the theorem then follows.

Part (ii): Recall that $Z^{(M)} := \{Z_k\}_{k \in \mathcal{I}_M}$ are given by (55), where $g^{(M)} := \{g_k\}_{k \in \mathcal{I}_M}$ is a random field over G satisfying the mixing property (27), and that $Y^{(M)} := \{Y_k\}_{k \in \mathcal{I}_M}$ are given by (55), where $\tilde{g}^{(M)} := \{\tilde{g}_k\}_{k \in \mathcal{I}_M}$ are i.i.d. from the probability distribution π over G . Note that, differently to Part (i), we do not consider here a subset of indices.

For the i.i.d. measurements $Y^{(M)}$, we have the standard bias-variance decomposition

$$\text{MSE} \left(\hat{F}(Y^{(M)}) \right) = \mathbb{E} \left[\left\| \hat{F}(Y^{(M)}) - \mathcal{F}(X) \right\|^2 \right] = \text{bias}(\hat{F}(Y^{(M)}))^2 + \text{Var}(\hat{F}(Y^{(M)})),$$

where the bias of the estimator is defined as $\text{bias}(\widehat{F}(Y^{(M)})) = \left\| \mathbb{E}[\widehat{F}(Y^{(M)})] - \mathcal{F}(X) \right\|$. Since $\widehat{F}(Y^{(M)})$ is an i.i.d. average, we have

$$\text{bias}(\widehat{F}(Y^{(M)})) = \text{bias}(F(Y_1)) \quad \text{and} \quad \text{Var}(\widehat{F}(Y^{(M)})) = \frac{1}{|\mathcal{I}_M|} \text{Var}(F(Y_1)).$$

We assumed that the MSE with i.i.d. data vanishes (for fixed σ) as $M \rightarrow \infty$, which implies that the bias is zero with i.i.d. data. This implies in particular that $\mathbb{E}[F(Y_1)] = \mathcal{F}(X)$.

Now, for the dependent data $Z^{(M)}$, we can estimate the bias of the estimator $\widehat{F}(Z^{(M)})$ as

$$(59) \quad \text{bias}(\widehat{F}(Z^{(M)})) = \left\| \frac{1}{|\mathcal{I}_M|} \sum_{k \in \mathcal{I}_M} (\mathbb{E}[F(Z_k)] - \mathcal{F}(X)) \right\| \leq \frac{1}{|\mathcal{I}_M|} \sum_{k \in \mathcal{I}_M} \|\mathbb{E}[F(Z_k)] - \mathbb{E}[F(Y_1)]\|.$$

Since each Z_k has the same probability as Y_1 up to the distribution of the group element g_k , we have

$$\mathbb{E}[F(Z_k) | g_k = \eta] = \mathbb{E}[F(Y_1) | \tilde{g}_1 = \eta], \quad \forall \eta \in G,$$

and using the mixing property (27), we can write

$$\begin{aligned} \|\mathbb{E}[F(Z_k)] - \mathbb{E}[F(Y_1)]\| &= \left\| \sum_{\eta \in G} \mathbb{P}(g_k = \eta) \mathbb{E}[F(Z_k) | g_k = \eta] - \sum_{\eta \in G} \pi(\eta) \mathbb{E}[F(Y_1) | g_1 = \eta] \right\| \\ &\leq \sum_{\eta \in G} |\mathbb{P}(g_k = \eta) - \pi(\eta)| \|\mathbb{E}[F(Y_1) | \tilde{g}_1 = \eta]\| \\ &\leq C \exp(-\gamma \text{dist}(\{k\}, \mathcal{I}_M^c)), \end{aligned}$$

for some constant C . Due to the exponential decay of $\exp(-\gamma \text{dist}(\{k\}, \mathcal{I}_M^c))$ as $M \rightarrow \infty$, we have

$$\lim_{M \rightarrow \infty} \sum_{k \in \mathcal{I}_M} C \exp(-\gamma \text{dist}(\{k\}, \mathcal{I}_M^c)) = K_1,$$

for some $K_1 > 0$. Hence, (59) implies

$$(60) \quad \limsup_{M \rightarrow \infty} |\mathcal{I}_M| \text{bias}(\widehat{F}(Z^{(M)})) \leq K_1.$$

It remains to control the variance of $\widehat{F}(Z^{(M)})$.

We can write

$$\begin{aligned} (61) \quad \left| \text{Var}(\widehat{F}(Z^{(M)})) - \text{Var}(\widehat{F}(Y^{(M)})) \right| &= \left| \frac{1}{|\mathcal{I}_M|^2} \sum_{(i,j) \in \mathcal{I}_M^2} \text{Cov}(F(Z_i), F(Z_j)) - \text{Var}(\widehat{F}(Y^{(M)})) \right| \\ &\leq \left| \frac{1}{|\mathcal{I}_M|^2} \sum_{i \in \mathcal{I}_M} \text{Var}(F(Z_i)) - \text{Var}(\widehat{F}(Y^{(M)})) \right| \\ &\quad + \frac{1}{|\mathcal{I}_M|^2} \sum_{\substack{(i,j) \in \mathcal{I}_M^2 \\ i \neq j}} |\text{Cov}(F(Z_i), F(Z_j))|. \end{aligned}$$

Since $Y^{(M)} = \{Y_i\}_{1 \leq i \leq M^d}$ are i.i.d., we have

$$\begin{aligned} \left| \frac{1}{|\mathcal{I}_M|^2} \sum_{i \in \mathcal{I}_M} \text{Var}(F(Z_i)) - \text{Var}(\widehat{F}(Y^{(M)})) \right| &= \left| \frac{1}{|\mathcal{I}_M|^2} \sum_{i \in \mathcal{I}_M} (\text{Var}(F(Z_i)) - \text{Var}(F(Y_1))) \right| \\ &\leq \frac{1}{|\mathcal{I}_M|^2} \sum_{i \in \mathcal{I}_M} |\text{Var}(F(Z_i)) - \text{Var}(F(Y_1))| \end{aligned}$$

Due to the mixing property (27), $|\text{Var}(F(Z_i)) - \text{Var}(F(Y_1))| \rightarrow 0$ as the distance of the index i from the boundary of \mathcal{I}_M goes to infinity, which implies that

$$\lim_{M \rightarrow \infty} \frac{1}{|\mathcal{I}_M|} \sum_{i \in \mathcal{I}_M} |\text{Var}(F(Z_i)) - \text{Var}(F(Y_1))| = 0.$$

Hence,

$$(62) \quad \lim_{M \rightarrow \infty} |\mathcal{I}_M| \left| \frac{1}{|\mathcal{I}_M|^2} \sum_{i \in \mathcal{I}_M} \text{Var}(F(Z_i)) - \text{Var}(\widehat{F}(Y^{(M)})) \right| = 0.$$

Next, we prove that, for any $(i, j) \in \mathcal{I}_M^2$ with $i \neq j$, it holds that

$$(63) \quad \left| \mathbb{E}[F(Z_i)F(Z_j)] - \mathbb{E}[F(Y_1)]^2 \right| \leq C \exp(-\gamma \min\{|i - j|, \text{dist}(\{i, j\}, \mathcal{I}_M^c)\}).$$

for some constant $C > 0$, and for γ as in Assumption 5.5.

First, we note that since Y_i and Y_j are i.i.d., we have $\mathbb{E}[F(Y_i)F(Y_j)] = \mathbb{E}[F(Y_1)]^2$, for all $i \neq j$. Moreover, since the distribution of Z_i, Z_j and Y_i, Y_j are equal up to the distribution of the associated group actions, we have that

$$\mathbb{E}[F(Z_i)F(Z_j)|g_i = \eta_i, g_j = \eta_j] = \mathbb{E}[F(Y_i)F(Y_j)|\tilde{g}_i = \eta_i, \tilde{g}_j = \eta_j], \quad \forall \eta_i, \eta_j \in G.$$

Therefore, we have that

$$\begin{aligned} (64) \quad \mathbb{E}[F(Z_i)F(Z_j)] &= \mathbb{E}[F(Z_i)F(Z_j) - F(Y_i)F(Y_j)] + \mathbb{E}[F(Y_1)]^2 \\ &= \sum_{\eta_i, \eta_j} (\mathbb{P}[g_i = \eta_i, g_j = \eta_j] - \pi(\eta_i)\pi(\eta_j)) \mathbb{E}[F(Z_i)F(Z_j)|g_i = \eta_i, g_j = \eta_j] \\ &\quad + \mathbb{E}[F(Y_1)]^2. \end{aligned}$$

Now, we can use the formula for conditional probabilities and the mixing property (27) to obtain

$$\begin{aligned} |\mathbb{P}[g_i = \eta_i, g_j = \eta_j] - \pi(\eta_i)\pi(\eta_j)| &= |\mathbb{P}[g_i = \eta_i | g_j = \eta_j] \mathbb{P}[g_j = \eta_j] - \pi(\eta_i)\pi(\eta_j)| \\ &\leq \mathbb{P}(g_j = \eta_j) |\mathbb{P}[g_i = \eta_i | g_j = \eta_j] - \pi(\eta_i)| \\ &\quad + \pi(\eta_i) |\mathbb{P}[g_j = \eta_j] - \pi(\eta_j)| \\ &\leq 2c_1 \exp(-\gamma \min\{|i - j|, \text{dist}(\{i, j\}, \mathcal{I}_M^c)\}) \end{aligned}$$

Plugging this estimate in (64), we obtain (63). Similarly, one can prove that

$$(65) \quad \left| \mathbb{E}[F(Z_i)] \mathbb{E}[F(Z_j)] - \mathbb{E}[F(Y_1)]^2 \right| \leq C \exp(-\gamma \min\{|i - j|, \text{dist}(\{i, j\}, \mathcal{I}_M^c)\}),$$

for all $i \neq j$.

Using (63) and (65), we can estimate $\text{Cov}(F(Z_i), F(Z_j))$ as

$$\begin{aligned}
 |\text{Cov}(F(Z_i), F(Z_j))| &= |\mathbb{E}[F(Z_i)F(Z_j)] - \mathbb{E}[F(Z_i)]\mathbb{E}[F(Z_j)]| \\
 &\leq \left| \mathbb{E}[F(Z_i)F(Z_j)] - \mathbb{E}[F(Y_1)]^2 \right| \\
 &\quad + \left| \mathbb{E}[F(Y_1)]^2 - \mathbb{E}[F(Z_i)]\mathbb{E}[F(Z_j)] \right| \\
 (66) \quad &\leq 2C \exp(-\gamma \min\{d(i, j), \text{dist}(\{i, j\}, \mathcal{I}_M^c)\}).
 \end{aligned}$$

Due to the exponential decay with respect to the distance, for every fixed $i_0 \in \mathcal{I}_M$, we have

$$\sum_{\substack{j \in \mathcal{I}_M \\ j \neq i_0}} 2C \exp(-\gamma \min\{d(i_0, j), \text{dist}(\{i_0, j\}, \mathcal{I}_M^c)\}) \leq K_2,$$

for some $K_2 > 0$ independent of M . Hence, from (66) we obtain

$$(67) \quad \frac{1}{|\mathcal{I}_M|^2} \sum_{\substack{(i, j) \in \mathcal{I}_M^2 \\ i \neq j}} |\text{Cov}(F(Z_i), F(Z_j))| \leq \frac{1}{|\mathcal{I}_M|^2} \sum_{i \in \mathcal{I}_M} K_2 = \frac{K_2}{|\mathcal{I}_M|}.$$

Then, combining (62) and (67) with (61), we obtain

$$\limsup_{M \rightarrow \infty} |\mathcal{I}_M| \left| \text{Var}(\widehat{F}(Z^{(M)})) - \text{Var}(\widehat{F}(Y^{(M)})) \right| \leq K_2.$$

The fact that $\text{bias}(\widehat{F}(Y^{(M)})) = 0$ together with (60) imply that

$$\limsup_{M \rightarrow \infty} |\mathcal{I}_M| \left| \text{bias}(\widehat{F}(Z^{(M)})) - \text{bias}(\widehat{F}(Y^{(M)})) \right| \leq K_1.$$

Hence, using the bias variance decomposition

$$\text{MSE}(\widehat{F}(Z^{(M)})) = \text{bias}(\widehat{F}(Z^{(M)}))^2 + \text{Var}(\widehat{F}(Z^{(M)})),$$

we obtain

$$\limsup_{M \rightarrow \infty} |\mathcal{I}_M| \left| \text{MSE}(\widehat{F}(Z^{(M)})) - \text{MSE}(\widehat{F}(Y^{(M)})) \right| \leq \|F\|_\infty K_1 + K_2,$$

which, in view of the convergence rate of $\widehat{F}(Y^{(M)})$ and the assumption $a(\sigma) \geq \tau > 0$, implies

$$\limsup_{M \rightarrow \infty} \frac{\text{MSE}(\widehat{F}(Z^{(M)}))}{\frac{a(\sigma)}{|\mathcal{I}_M|}} \leq \frac{\|F\|_\infty K_1 + K_2}{a(\sigma)} + \limsup_{M \rightarrow \infty} \frac{\text{MSE}(\widehat{F}(Y^{(M)}))}{\frac{a(\sigma)}{|\mathcal{I}_M|}} \leq \frac{\|F\|_\infty K_1 + K_2}{\tau} + 1,$$

and the conclusion follows. □

KWEKU ABRAHAM
DEPARTMENT OF APPLIED MATHEMATICS AND THEORETICAL PHYSICS
UNIVERSITY OF CAMBRIDGE
WILBERFORCE ROAD, CB3 0WA
CAMBRIDGE, UNITED KINGDOM

Email address: lkwa2@cam.ac.uk

AMNON BALANOV AND TAMIR BENDORY
SCHOOL OF ELECTRICAL AND COMPUTER ENGINEERING
TEL AVIV UNIVERSITY
TEL AVIV, ISRAEL

Email address: amnonba15@gmail.com

Email address: bendory@tauex.tau.ac.il

CARLOS ESTEVE-YAGÜE
DEPARTAMENTO DE MATEMÁTICAS
UNIVERSIDAD DE ALICANTE
03690 SAN VICENTE DEL RASPEIG
ALICANTE, SPAIN

Email address: c.esteve@ua.es